Physical and functional interaction between the α- and γ-secretases: A new model of regulated intramembrane proteolysis

Physical and functional interaction between the α- and γ-secretases: A new model of regulated intramembrane proteolysis

Allen C. Chen,[1] Sumin Kim,[1] Nina Shepardson,[1] Sarvagna Patel,[1] Soyon Hong,[2] and Dennis J. Selkoe[1]

[1]Ann Romney Center for Neurologic Diseases, Brigham and Women's Hospital and [2]Department of Neurology, F.M. Kirby Neurobiology Center, Boston Children's Hospital, Harvard Medical School, Boston, MA 02115

Many single-transmembrane proteins are sequentially cleaved by ectodomain-shedding α-secretases and the γ-secretase complex, a process called regulated intramembrane proteolysis (RIP). These cleavages are thought to be spatially and temporally separate. In contrast, we provide evidence for a hitherto unrecognized multiprotease complex containing both α- and γ-secretase. ADAM10 (A10), the principal neuronal α-secretase, interacted and cofractionated with γ-secretase endogenously in cells and mouse brain. A10 immunoprecipitation yielded γ-secretase proteolytic activity and vice versa. In agreement, superresolution microscopy showed that portions of A10 and γ-secretase colocalize. Moreover, multiple γ-secretase inhibitors significantly increased α-secretase processing ($r = -0.86$) and decreased β-secretase processing of β-amyloid precursor protein. Select members of the tetraspanin web were important both in the association between A10 and γ-secretase and the γ→α feedback mechanism. Portions of endogenous BACE1 coimmunoprecipitated with γ-secretase but not A10, suggesting that β- and α-secretases can form distinct complexes with γ-secretase. Thus, cells possess large multiprotease complexes capable of sequentially and efficiently processing transmembrane substrates through a spatially coordinated RIP mechanism.

Introduction

In the late 1990s, a convergence of findings coming principally from molecular studies of cholesterol homeostasis and of Alzheimer's disease (AD) gave rise to a new concept in biochemistry: regulated intramembrane proteolysis (RIP; Brown et al., 2000). Ensuing research led to the recognition of RIP as a universal signaling mechanism conserved from bacteria to humans. RIP involves the cleavage of diverse transmembrane proteins within the hydrophobic bilayer, resulting in the release of water-soluble fragments, many of which are essential for cellular signaling. Such proteolytic events are now known to be catalyzed by one of several intramembrane proteases that include Rhomboid, site-2 protease (S2P), γ-secretase, and signal peptide peptidase. RIP often begins with an initial proteolytic cleavage that sheds the soluble ectodomain of the transmembrane substrate, allowing subsequent cleavage by the respective intramembrane proteases.

Perhaps the most studied of the intramembrane proteases is the γ-secretase complex, a highly conserved signaling hub that processes a large and growing list of single transmembrane proteins that function in diverse biological pathways ranging from development to neurodegeneration (Jurisch-Yaksi et al., 2013). Cleavage of one such substrate, Notch, is required for cell fate determinations in metazoans (De Strooper et al., 1999; Greenwald, 2012), and the processing of another substrate, β-amyloid precursor protein (APP), generates the neurotoxic amyloid β-peptide (Aβ) centrally implicated in AD (Hardy and Selkoe, 2002). Aβ is generated normally when APP undergoes shedding of its N-terminal ectodomain (amyloid precursor protein soluble–β [APPs-β]) by β-secretase, leaving a C-terminal stub (C99) that is then cleaved by γ-secretase within its transmembrane domain (TMD) to release Aβ and the APP intracellular domain (AICD; Fig. 1 A). Because it generates Aβ, γ-secretase is a target for the development of inhibitors to treat AD. Several γ-secretase inhibitors have reached human testing. However, these trials have met with complications because

Correspondence to Dennis J. Selkoe: dselkoe@rics.bwh.harvard.edu

Abbreviations used in this paper: A10, ADAM10; Aβ, amyloid β-peptide; AD, Alzheimer's disease; ADAM, a disintegrin and metalloproteinase; AICD, APP intracellular domain; ANOVA, analysis of variance; APP, β-amyloid precursor protein; BACE1, beta-site APP-cleaving enzyme 1; BN-PAGE, blue native PAGE; CHAPSO, 3-([3-cholamidopropyl]dimethylammonio)-2-hydroxy-1-propanesulfonate; CM, conditioned media; coIP, coimmunoprecipitation; CTF, C-terminal transmembrane fragment; DDM, *n*-dodecyl β-D-maltoside; FAD, familial AD; FLIM, fluorescence lifetime imaging microscopy; FRET, fluorescence resonance energy transfer; HMW, high molecular weight; IP, immunoprecipitation; LMW, low molecular weight; MSD, meso scale discovery; NCT, Nicastrin; NPR A, natriuretic peptide receptor A; NTF, N-terminal transmembrane fragment; PAA, protein A agarose; PCC, Pearson correlation coefficient; PS, Presenilin; RIP, regulated intramembrane proteolysis; SEC, size-exclusion chromatography; SIM, structured illumination microscopy; TACE, TNF-converting enzyme; TFR, transferrin receptor; TSPAN, tetraspanin; WB, Western blotting; WT, wild type.

The Rockefeller University Press $30.00
J. Cell Biol. Vol. 211 No. 6 1157–1176
www.jcb.org/cgi/doi/10.1083/jcb.201502001

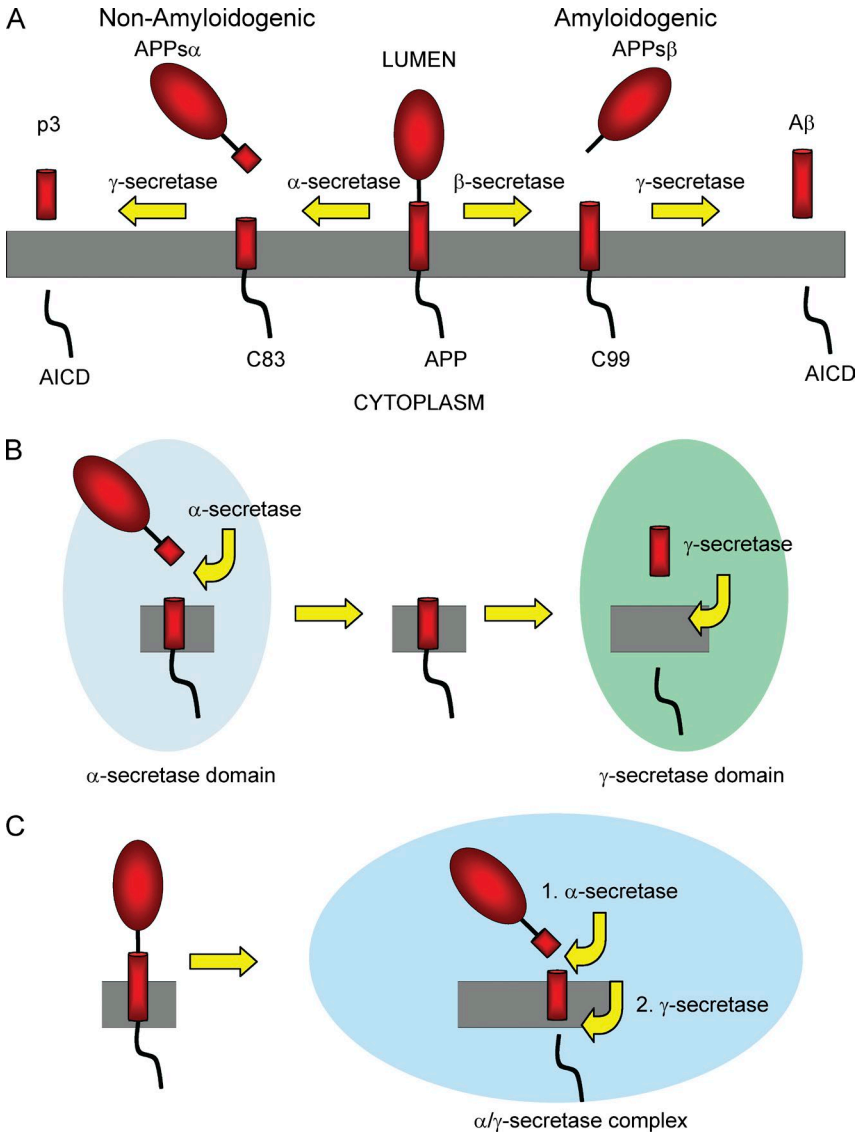

Figure 1. **Models of APP processing by the various secretases.** (A) Processing of APP by α-, β-, and γ-secretases. (B) Current model of γ-secretase substrate processing in which the ectodomain shedding and the intramembrane cleavages are assumed to be separated spatially and temporally. (C) Proposed new model of γ-secretase processing based on all data herein in which the principal sheddase (α-/β-secretase) exists in an HMW complex with γ-secretase that accepts full-length substrates for rapid sequential processing.

γ-secretase normally processes many substrates besides APP, as shown by the failure of semagacestat (Doody et al., 2013).

Although much attention has focused on the APP amyloidogenic pathway just described, APPs (and many other γ-secretase substrates) are predominantly processed by an alternate pathway involving ectodomain shedding by an α-secretase, followed by constitutive γ-secretase cleavage. In the example of APP, α-secretase cleaves within the Aβ region, liberating a slightly longer ectodomain (amyloid precursor protein soluble–alpha [APPs-α]) and leaving a shorter transmembrane stub (C83) that is then cleaved by γ-secretase to generate the small p3 peptide and AICD (Fig. 1 A). α-Secretase cleavage is usually performed by a member of the ADAM (a disintegrin and metalloproteinase) family, which processes many type I transmembrane substrates involved in myriad signaling pathways (Weber and Saftig, 2012). ADAM10 (A10) is the physiologically relevant α-secretase for ectodomain shedding of APP and other substrates in primary neurons and many cell lines (Kuhn et al., 2010). Regulated shedding by α-secretase via phorbol ester stimulation is likely catalyzed by TNF-converting enzyme (TACE, or ADAM17; Buxbaum et al., 1998).

Despite the wealth of information about the α-, β-, and γ-secretases individually, almost nothing is known about whether these proteases interact and whether there is a mechanism by which they regulate each other's activities. There are two general possibilities as to whether α- and γ-secretases coordinate their sequential activities. One model is the current assumption that the α- and γ-secretase cleavages are separated spatially and temporally in distinct membrane loci (Fig. 1 B). Such a mechanism would seem inefficient, as the hydrophobic C-terminal transmembrane fragments (CTFs) that are created by α- or β-secretase would have to traffic within the lipid bilayer to distinct membrane loci where γ-secretase resides for further processing. We hypothesized instead that the α- and γ-secretases are physically linked to facilitate sequential processing of substrates (Fig. 1 C). We based this new hypothesis in large part on our identification of Aph-1 as a docking site within the γ-complex for both full-length and ectodomain-shed substrates (Chen et al., 2010). It was unclear why full-length proteins, which are not the direct targets of γ-secretase, would interact with the γ-complex, unless only full-length substrates that are about to be processed by α-secretase enter a combined complex for efficient sequential processing. This hypothesis suggests that the sheddase and

γ-secretase may not be separated spatially but, rather, occur in the same physical complex. There is sparse emerging evidence that substrate processing by the different secretases may be more interconnected than thought heretofore. For example, an APP-based peptidomimetic inhibitor of γ-secretase (based on the transmembrane domain sequence just downstream of Aβ) inhibited γ processing of APP but also altered APP ectodomain shedding (Esselens et al., 2012). In addition, there is evidence that α-secretase may serve not only to remove the ectodomain of substrates, but also to "hand off" substrates to γ-secretase for processing (Hemming et al., 2008). When the C-terminal region of a nonsubstrate (integrin-β1) was fused to the large ectodomain of a γ substrate (vasorin), this chimeric substrate could be shed in cells by α-secretase, and the resultant α-CTF was then cleaved by γ-secretase. However, if only the α-CTF of this chimeric substrate was directly expressed, it could not be cleaved by γ-secretase. This finding raised the possibility that α processing may be required for the passing of a substrate on to γ-secretase and that having a permissive γ sequence is not sufficient to yield γ cleavage in cells.

Here, we examine in detail the concept that substrate processing by α- and γ-secretase is interrelated both physically and functionally. We identify a novel interaction of γ-secretase with A10. We propose a new model in which the α- and γ-secretases reside in a complex capable of accepting full-length substrates for efficient, sequential processing. This interaction, which we show, also applies to β-secretase (β-site APP-cleaving enzyme 1 [BACE1]) and may be extendable to other intramembrane proteases that require a prior cleavage event.

Results

γ-Secretase interacts with the α-secretases A10 and TACE at both overexpressed and endogenous levels, including on the plasma membrane

Although full-length substrates are not the immediate proteolytic targets of γ-secretase, we and others have obtained evidence that they can interact with the γ-complex (Xia et al., 1997b; Ray et al., 1999; Chen et al., 2010). On this basis, we hypothesized that the α- and γ-secretases may function together in a larger multimeric complex for efficient substrate processing. To determine whether α-secretase associates with γ-secretase, we initially examined our γ-30 cell line: CHO cells that stably overexpress human APP, three of the four human γ components (Presenilin1 [PS1], Aph-1, and Pen-2, but not Nicastrin [NCT]), and transferrin receptor (TFR; Kimberly et al., 2003). These cells express only endogenous A10 and TACE, the predominant α-secretases for APP. Each ADAM is synthesized as an inactive proprotein (immature) that undergoes a Furin-like cleavage leading to maturation. Mature TACE (but not mature A10) is highly unstable after cell lysis (Schlöndorff et al., 2000) but can be detected well when cells are lysed in the presence of a metalloprotease inhibitor like 1,10-phenanthroline (Fig. 2 A, compare lanes 1 and 2). By enriching for γ-secretase via Aph-1 immunoprecipitation (IP) of lysates made in 1% 3-([3-cholamidopropyl]dimethylammonio)-2-hydroxy-1-propanesulfonate (CHAPSO; one of the few detergents that leaves the γ-complex intact), we detected the coimmunoprecipitation (coIP) of A10 and TACE (Fig. 2 A, lanes 3 and 4). Next, we performed coIPs in the reverse direction: A10 immunoprecipitates were probed for the coIP of PS1 CTF, and as a control, lysates were immunoprecipitated for the known non–γ substrate natriuretic peptide receptor A (NPR A; Hemming et al., 2008). We observed coIP of γ-secretase (PS1 CTF) only in the A10 immunoprecipitates (Fig. 2 B). To rule out nonspecific protein interaction after lysis, lysates of cells that contained no γ-secretase (α+, γ−; Fig. 2 C, lane 1) and lysates of cells that contained no A10 (α−, γ+; Fig. 2 C, lane 2) were mixed (Mix 1; Fig. 2 C, lane 5) and immunoprecipitated for γ-secretase (see Sample preparation and IP in Materials and methods for details). We saw no coIP of A10 (Fig. 2 C, lane 7), even though there were significant levels of A10 in the starting mix (Fig. 2 C, lanes 1 and 5). As a positive control for this experiment, lysates that contained neither A10 nor γ-secretase (α−, γ−; Fig. 2 C, lane 3) or lysates that contained both proteases (α+, γ+; Fig. 2 C, lane 4) were mixed and immunoprecipitated for γ-secretase. We observed a robust coIP of A10 with the γ components (Fig. 2 C, lane 8). Together, these control experiments indicate that the association between A10 and γ-secretase is not a result of nonspecific postlysis interaction, but occurs within cells.

Next, we sought to establish that the secretases can interact at the plasma membrane where they are known to be proteolytically active (Gutwein et al., 2003; Chyung et al., 2005) and involved in many forms of cell signaling. Live γ-30 cells were treated with a nonpenetrant biotinylation reagent (or not) at 4°C to label surface proteins. Surface-biotinylated and control cell lysates were enriched for intact γ-secretase by IP of Aph-1, an early member in γ-complex assembly (LaVoie et al., 2003). The resultant immunoprecipitates were subjected to streptavidin pull-down to enrich for cell surface interactors of γ-secretase. Aph-1 coimmunoprecipitated both immature and mature endogenous A10; however, mostly mature A10 was detected in the subsequent streptavidin pull-down, suggesting that mature A10 interacts with γ-secretase at the CHO cell surface (Fig. 2 D). As a control for proper cell surface labeling, no immature NCT (ER localized) was detected in the streptavidin pull-down (Fig. 2 D, lane 6). A similar coimmunoprecipitate was observed for TACE: only the mature form was recovered with γ-secretase at the cell surface (Fig. S1 A). Immunoprecipitating γ-secretase via Pen-2 (the last component of γ-secretase to join the complex) enriched predominantly for mature γ-complexes (as opposed to immature), and at the cell surface, the biotinylated γ-complex was associated with biotinylated mature A10 (Fig. S1 B). Thus, portions of mature α- and γ-secretases interact at the plasma membrane, a location where each has been shown to be active.

We sought to validate the interaction of γ-secretase with A10 and TACE under solely endogenous expression. Using 7W CHO cells, the parental line of the γ-30 cells that expresses only endogenous γ components, we detected coIP of active, mature γ-secretase (i.e., PS1 N-terminal transmembrane fragment [NTF]/CTF) when 7W lysates made in the presence of phenanthroline were immunoprecipitated for endogenous TACE using two different antibodies, whereas protein A agarose (PAA) beads alone brought down no γ-secretase components (Fig. 3 A). However, in the absence of phenanthroline, very little mature TACE was present and immunoprecipitated, and the levels of PS1 CTF that coimmunoprecipitated were correspondingly very low (Fig. 3 A, lanes 5 and 7). This selectivity of endogenous PS1 binding to endogenous mature but not immature TACE (although the two forms are closely similar transmembrane polypeptides) supports the specificity of our coIP. Thus, in 7W cells, endogenous mature TACE can interact

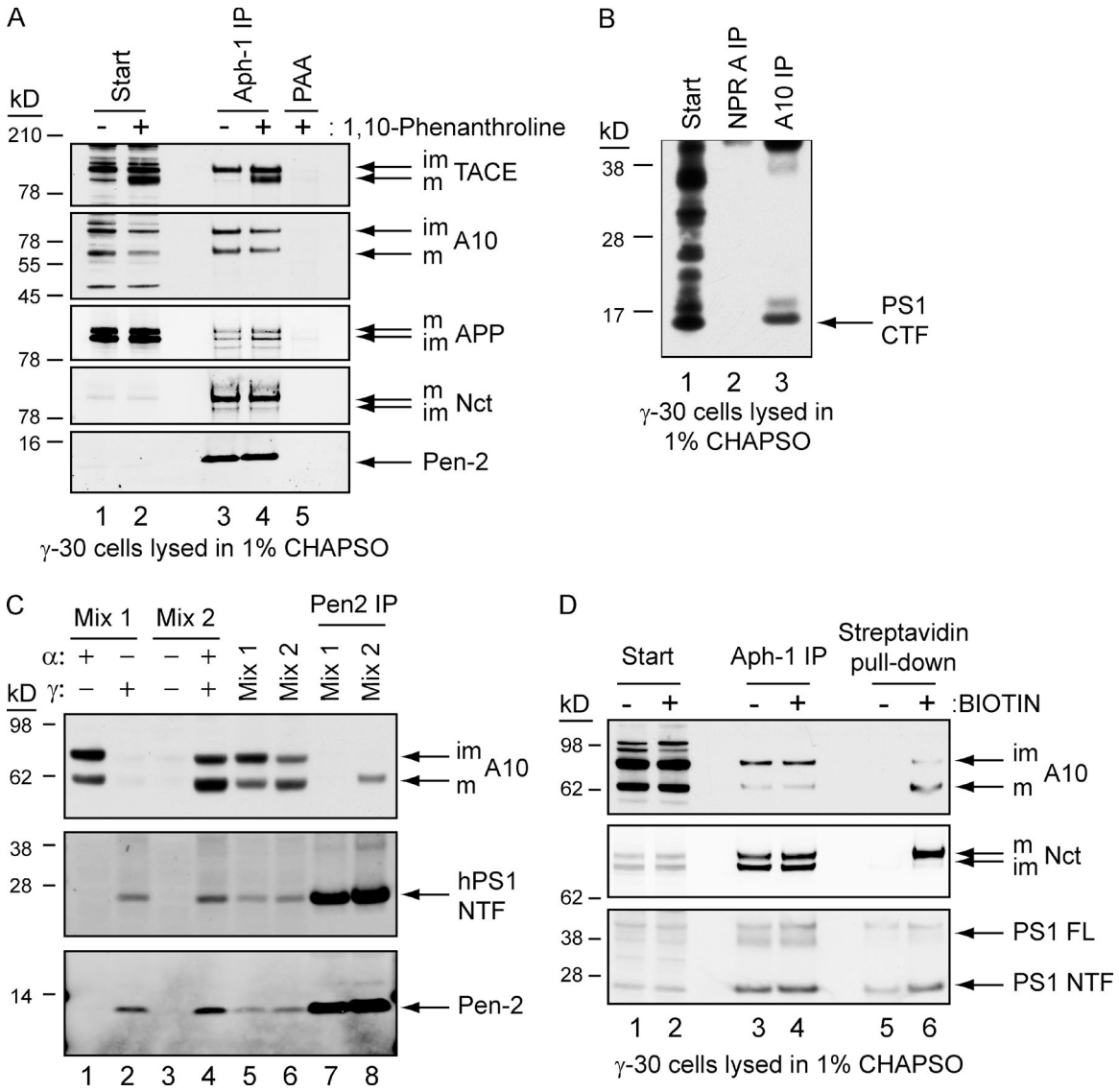

Figure 2. **The α-secretases A10 and TACE interact with γ-secretase at overexpressed levels and at the plasma membrane.** (A) CHAPSO-solubilized lysates of γ-30 CHO cells were immunoprecipitated for Aph-1 or PAA as a control in the absence or presence of the metalloprotease inhibitor 1,10-phenanthroline. Immunoprecipitates were blotted to probe for coIP of A10 or TACE, APP, and for the γ components NCT and Pen-2. (B) γ-30 lysates were immunoprecipitated for either A10 or NPR A as a control. Resulting immunoprecipitates were probed for the coIP of PS1 CTF. (C) Lysates from cells that express A10 only, human γ-secretase only, neither, or both (lanes 1, 2, 3, and 4, respectively) were specifically pooled to form mix 1 (A10 only + γ-secretase only) or mix 2 (neither + both) and then immunoprecipitated for γ-secretase with an M2 resin targeting the Flag tag on Pen-2. Immunoprecipitates were probed for the coIP of A10 and the γ components PS1 NTF and Pen-2. (D) γ-30 cells were treated with a nonpermeable biotinylation reagent at 4°C to label cell surface proteins. Lysates were immunoprecipitated for Aph-1, and the resultant immunoprecipitates were eluted and pulled down with streptavidin to enrich for cell surface interactors of γ-secretase, followed by blotting for α- and γ-secretases as in A. im, immature; m, mature.

in part with endogenous γ-secretase. Next, we asked whether this interaction was conserved in the human neuroblastoma cell line, M17D. These cells have high levels of both mature and immature A10 but no detectable mature TACE (only immature). When M17D cells were lysed in the presence of phenanthroline and immunoprecipitated for A10 or TACE, we observed clear coIP of PS1 NTF and CTF with A10 but virtually no interaction with TACE (Fig. 3 B), suggesting that in these neural cells, an endogenous A10–γ-secretase complex is more abundant than a TACE–γ-secretase complex, presumably as a result of the low level of mature TACE endogenously (Fig. 3 B).

To confirm the interaction in a more physiological system, we prepared microsomes from wild-type (WT) adult mouse brain and solubilized them in 1% CHAPSO, immunoprecipitated for A10 with two distinct antibodies, and blotted for coIP of PS1 CTF (Fig. 3 C). We observed coIP of γ-secretase with mature A10 in this tissue, further supporting that the interaction is physiological. Next, we asked whether other ADAM members interact with γ-secretase in brain. Mouse brain microsomes were immunoprecipitated for ADAM9, TACE, or A10 and blotted for PS1 CTF. In brain, as in M17D cells, we observed mostly immature TACE and detected no coIP of γ-secretase with the TACE antibody (Fig. 3, D and E). Likewise, we did not observe any coIP of PS1 CTF by ADAM9 IP (Fig. 3 D). These results provide important specificity controls for our co-immunoprecipitates: only immunoprecipitating for A10 among these three type I transmembrane proteins consistently brought down endogenous PS1 CTF from normal brain (Fig. 3, D and

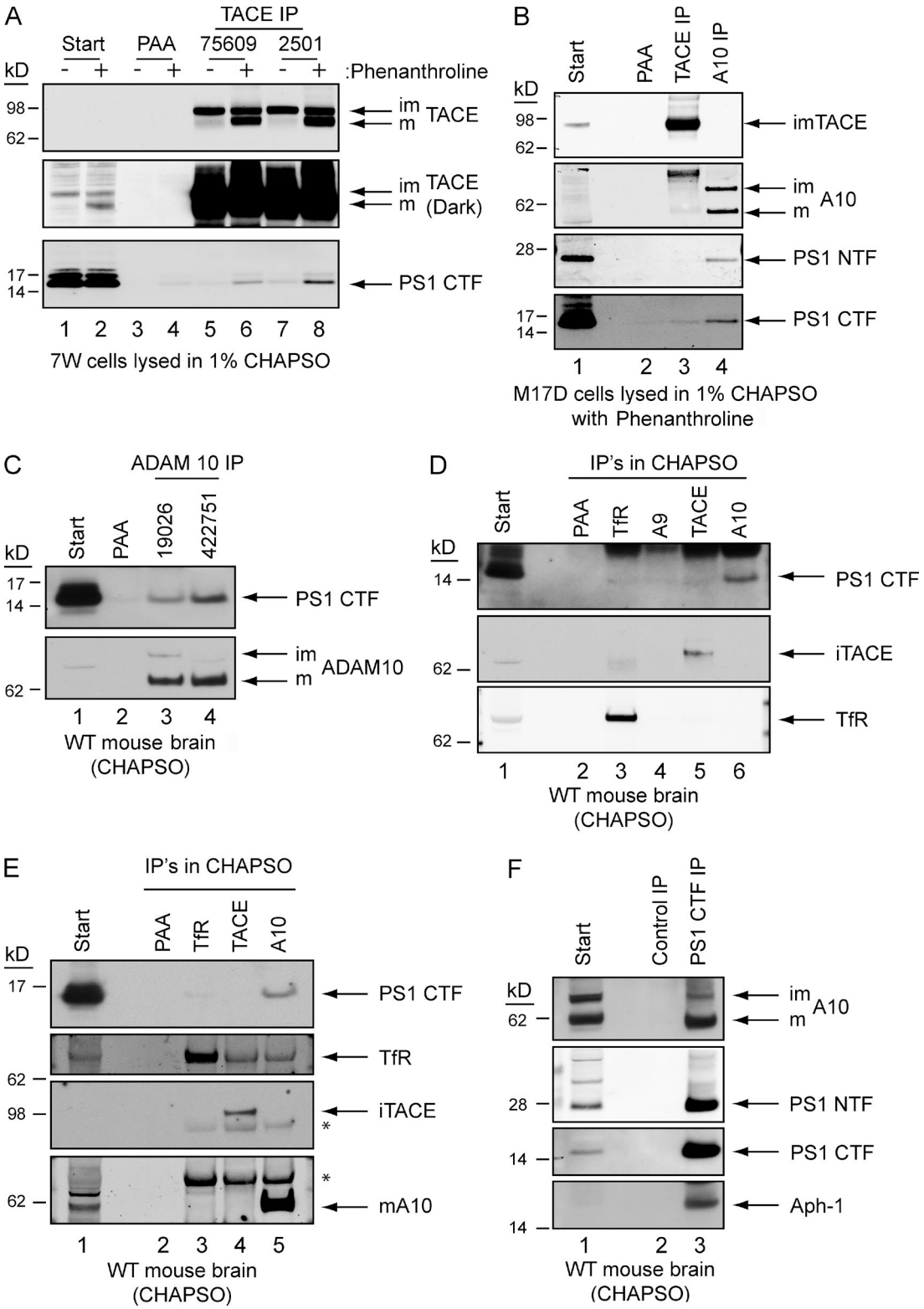

Figure 3. **The association between A10 and γ-secretase is observed at endogenous expression levels in cells and WT mouse brain.** (A) 7W cells were lysed in 1% CHAPSO in the absence or presence of 1,10-phenanthroline, immunoprecipitated for TACE or just with PAA, and then probed for coIP of PS1 CTF. (B) M17D cells were lysed in CHAPSO with 1,10-phenanthroline. Lysates were immunoprecipitated for TACE or A10 and probed for coIP of PS1 CTF. (C) Microsomes prepared from WT mouse brains were immunoprecipitated for A10 with two different antibodies (19026 and 422751) and blotted for the coIP of PS1 CTF. (D and E) Mouse brain microsomes were immunoprecipitated for TACE, A10, or ADAM9 (A9) and controls of PAA only or TFR and probed for coIP of PS1 CTF, TFR, TACE, and A10. The asterisks indicate nonspecific bands. (F) Mouse brain microsomes were immunoprecipitated for PS1 CTF and blotted for coIP of A10, PS1, and APH-1. im, immature; m, mature.

E). As a further control for specificity, IP of TFR, a type II protein that does not interact with γ-secretase, brought down very little or no PS1 CTF (Fig. 3, D and E). These multiple controls indicate that the interaction between A10 and γ-secretase is not a result of nonspecific interactions between membrane proteins. Next, we immunoprecipitated for PS1 in the mouse brain microsomes and blotted for A10. We detected interaction with A10 in this reverse direction; importantly, we again observed principally mature A10 interacting with the components of γ-secretase (Fig. 3 F), supporting the conclusion that under entirely endogenous conditions, mature γ-secretase can associate with mature α-secretase.

Mature A10 and mature γ-secretase coexist in a high molecular weight (HMW) complex

The γ-secretase complex has been variably sized to be ∼250 to >2,000 kD, depending on the techniques used (Yu et al., 1998; Edbauer et al., 2002; Evin et al., 2005; Osenkowski et al., 2009). To determine whether A10 exists in an HMW complex that also contains γ-secretase endogenously, we fractionated microsomes isolated from WT mouse brains on a Superose 6 gel-filtration column. Mature A10 was present in HMW complexes (>2 MD) that cofractionated well with mature γ-complexes (Fig. 4 A). Importantly, previous use of a Superose 6 column also showed that γ-secretase fractionated in an HMW complex of ∼2 MD (Li et al., 2000). Immature A10 predominantly eluted in much smaller complexes (<90 kD) that did not fractionate well with mature γ-secretase (Fig. 4 A). In another size-exclusion chromatography (SEC) run, we pooled fractions containing HMW proteins (∼2 MD; fractions 5–9) or low molecular weight (LMW) proteins (<90 kD; fractions 20–24) and immunoprecipitated each pool for A10. Only the HMW fractions showed the coIP of mature γ-complexes (i.e., PS1 CTF and mature NCT) with mature A10 (Fig. 4 B, lane 4). A10 IP of the LMW fractions from the same SEC run brought down neither PS1 CTF nor mature NCT (Fig. 4 B, lane 5). These gel filtration experiments under native conditions demonstrate that a portion of mature A10 exists in an HMW complex with mature γ-secretase in normal brain.

Next, we performed blue native PAGE (BN-PAGE) on S20 cells lysed in *n*-dodecyl β-D-maltoside (DDM) detergent. When we probed for γ-secretase components, we observed that they comigrated at ∼440 kD (Fig. 4 C), which is consistent with a previous study (Edbauer et al., 2002). When we probed for A10, we observed bands at 440 kD and 240 kD, and both these bands were shown to be specific to A10 using siRNA (Fig. 4 D). The 440-kD A10 band comigrated with the HMW γ-secretase complex. We also observed similar data in 7W cells (endogenous γ-secretase; unpublished data). Together, these data suggest that A10 and γ-secretase comigrate in an HMW complex by two independent nondenaturing methods, SEC and BN-PAGE.

The α–γ-secretase complex is proteolytically active

To confirm that the α–γ-secretase complexes we observed were proteolytically active, we performed typical in vitro γ-secretase activity assays on α-secretase immunoprecipitates. We used a recombinant APP-based γ substrate (C100-Flag) and quantified the generation of AICD and Aβ by Western blotting (WB). A10 immunoprecipitates of S20 lysates, which coimmunoprecipitated mature γ-secretase (e.g., PS1 NTF) as before, mediated the processing of the C100 substrate to generate Aβ and AICD, confirming γ activity in the A10 pull-down (Fig. 5 A, lanes 5 and 6; quantification on the right). Aβ-specific ELISAs confirmed the production of Aβ seen on the Western blot (not depicted). As a simultaneous positive control, a γ activity assay that was performed on a direct IP of PS1 NTF produced even more abundant Aβ and AICD, as expected (Fig. 5 A, lanes 3 and 4). In the A10 IP, the C100 substrate underwent cleavage by A10 to a C83 fragment (Fig. 5 A, lanes 5 and 6); production of the latter was specifically inhibited by a known α-secretase inhibitor (TAPI-1; lanes 9 and 10). (That A10 can cleave C99 to C83 is documented [Kuhn et al., 2010].) The C83 fragment then underwent processing by γ-secretase, as a γ inhibitor increased its levels (Fig. 5 A, lanes 7 and 8), suggesting that sequential α–γ processing of the C100 substrate had occurred. However, we did not observe any processing of C99 to C83 in our PS1 IP (Fig. 5 A, lanes 3 and 4), likely because of the high levels of γ-secretase in those samples which may outcompete A10 for the C99 substrate; furthermore, the activity assay is optimized for γ-, not α-secretase activity, and the levels of α processing of C99 after a high enrichment of A10 (Fig. 5 A, lanes 5–8) were very low.

Next, we performed the reverse experiment: α-secretase activity assays were performed on γ-secretase IPs from the S20 cells. Here, we used as a substrate an internally quenched fluorogenic peptide designed for α-secretase–type metalloproteases that is unquenched upon cleavage. We immunoprecipitated for Flag–Pen-2 or Aph-1–HA (with M2 and 3F10 resins, respectively), and as negative controls, we immunoprecipitated for TFR (an irrelevant membrane protein also overexpressed in the S20 cells) or else with M2 resin preabsorbed with Flag peptide (Fig. 5 B). IP of Aph-1 (an early component in γ-secretase assembly) coimmunoprecipitated both mature and immature γ-complexes. However, IP of Pen-2 (the final component in γ assembly) coimmunoprecipitated mature γ-complexes (i.e., virtually all of the coimmunoprecipitated NCT was fully glycosylated; compare Aph-1 and Pen-2 lanes in Fig. 5 B). In agreement, Aph-1 pulled down predominantly immature A10, whereas Pen-2 coimmunoprecipitated almost exclusively mature A10 (Fig. 5 B). As hypothesized, both these γ immunoprecipitates yielded specific α-secretase activity (inhibitable by TAPI-1), whereas the negative controls (TFR IP or preabsorbed M2 IP) did not (quantified in Fig. 5 B, right). Together, these bidirectional coIPs indicate that the α–γ-secretase complex is proteolytically active, with each enzyme in the coprecipitated complex able to process substrate appropriately.

A10 partially colocalizes with γ-secretase by superresolution structured illumination microscopy (SIM) and fluorescence lifetime imaging

To support our biochemical findings, we first performed confocal immunofluorescence microscopy on 7W cells that express only endogenous α- and γ-secretases. Confocal imaging showed punctate staining for A10 and PS1 throughout the cell (Fig. 6 A), with the strongest colocalization near the cell periphery. To quantify the degree of colocalization between A10 and γ-secretase, we performed an unbiased, automated analysis to calculate the Pearson correlation coefficient (PCC; Fig. S2 C; Manders et al., 1992) and observed a PCC of 0.67 ± 0.08, whereas overlap between PS1 and a nonspecific single-transmembrane protein, TFR (Fig. S2 A), was significantly less

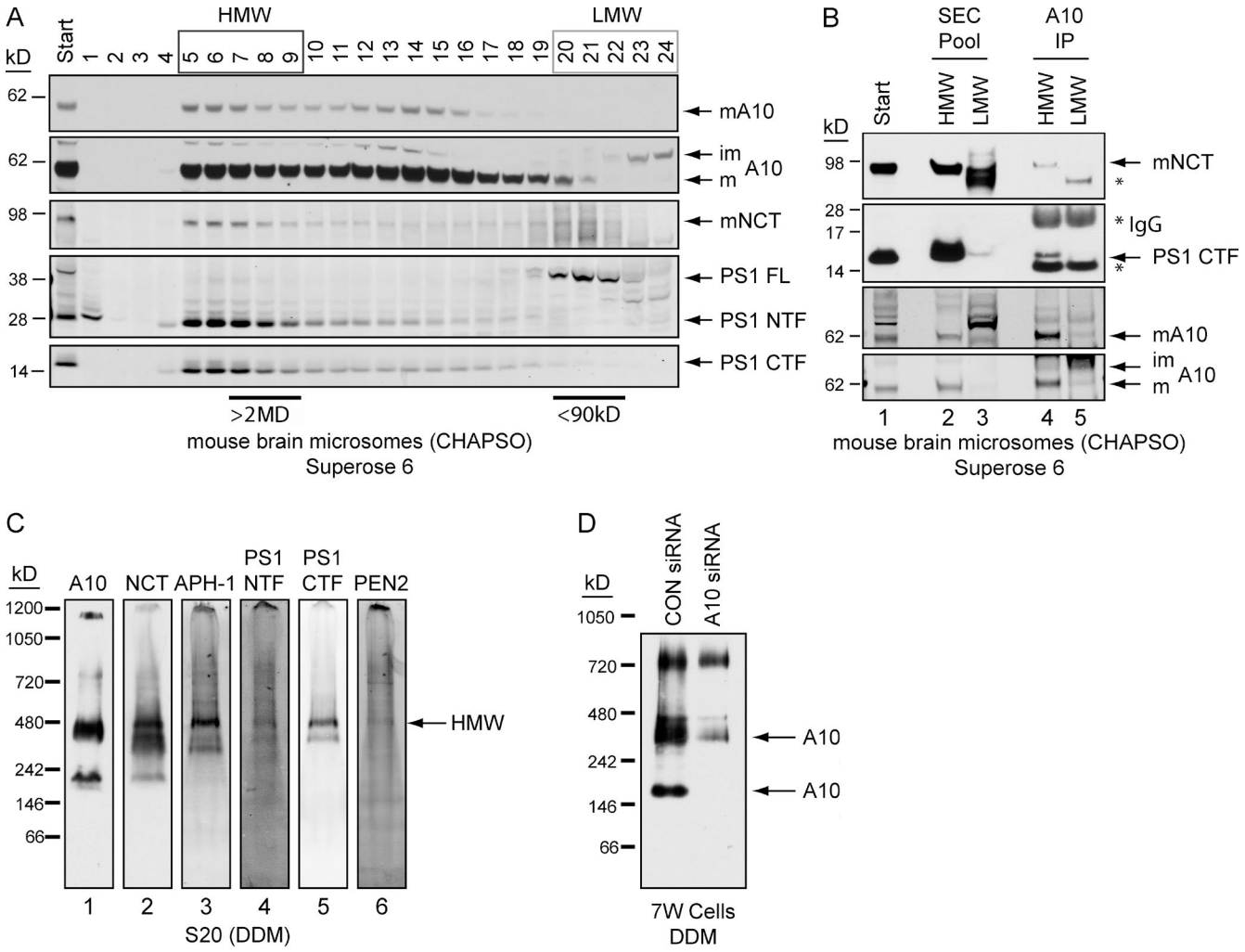

Figure 4. **A10 exists with γ-secretase in an HMW complex isolated from normal brain by SEC.** (A) WT mouse brain microsomes were fractionated on a Superose 6 column and blotted with antibodies to the indicated proteins. (B) Mouse brain microsome fractions from a Superose 6 column were pooled into HMW or LMW fractions and immunoprecipitated for A10 and then probed for A10 and coIP of NCT and PS1 CTF. The asterisks indicate nonspecific bands. (C) S20 cells were lysed in 0.25% DDM, loaded onto a BN-PAGE, and probed for A10 and γ-secretase. (D) 7W cells transfected with control or A10 siRNA were analyzed as in C. im, immature; m, mature.

at 0.35 ± 0.15, and overlap between A10 and TFR (Fig. S2 B) was 0.41 ± 0.11. These results suggest a high probability of colocalization of portions of A10 with PS at the cell surface, as expected from our biotinylation experiments (Fig. 2 D).

We performed superresolution imaging using SIM on our untransfected 7W cells. Consistent with our confocal data, SIM detected partial colocalization between A10 and PS1 at much higher resolutions (Fig. 6 B, orthogonal rendering after Imaris processing). We observed punctate staining of endogenous A10 and PS1 immunoreactivity throughout the cell body; however, the majority of colocalization occurred near the periphery of the cell, near the cell surface (Fig. 6 C, large view; Fig. 6 D, magnified image of inset in C; and Fig. 6 E, 3D rendering of C by Imaris). Next, we examined A10 and PS1 immunolocalization using SIM in intact hippocampal cryosections from young adult (3 mo old) C57BL/6 WT mice. SIM for PS1 and A10 in the stratum radiatum of the hippocampus revealed a punctate pattern (Fig. S2 D) that also colocalized with the postsynaptic marker Homer (not depicted), suggesting that A10 and PS1 may coexist at synaptic membranes. As a control, we also examined the colocalization of TFR with PS1 (Fig. S2 E) on the same brain tissue samples. To quantify colocalization between A10 and PS1, we analyzed images using Imaris and MAT LAB (see SIM section of Materials and methods). Analysis of the 3D SIM images revealed that 11.8% of total cellular A10-immunoreactive puncta colocalized with PS1-immunoreactive puncta versus 4.8% of total TFR-immunoreactive signal (Fig. S2 F). Therefore, our data using superresolution SIM demonstrate that a portion of A10 colocalizes with PS1 in cultured cells and in intact mouse brain tissue.

As a third imaging method to demonstrate colocalization, we measured the fluorescence lifetime of PS1 labeled with an Alexa Fluor 488 donor fluorophore in the absence or presence of A10 stained with a Cy3 acceptor fluorophore. Fluorescence lifetime imaging microscopy (FLIM) can be used to determine protein–protein proximity with <10 nm resolution (Lleó et al., 2004). When endogenous PS1 in 7W cells was labeled with Alexa Fluor 488 in the absence of an acceptor, we observed a lifetime of ~2,387 ± 39 ps, similar to what has been previously reported (Herl et al., 2009). In the presence of the CY3

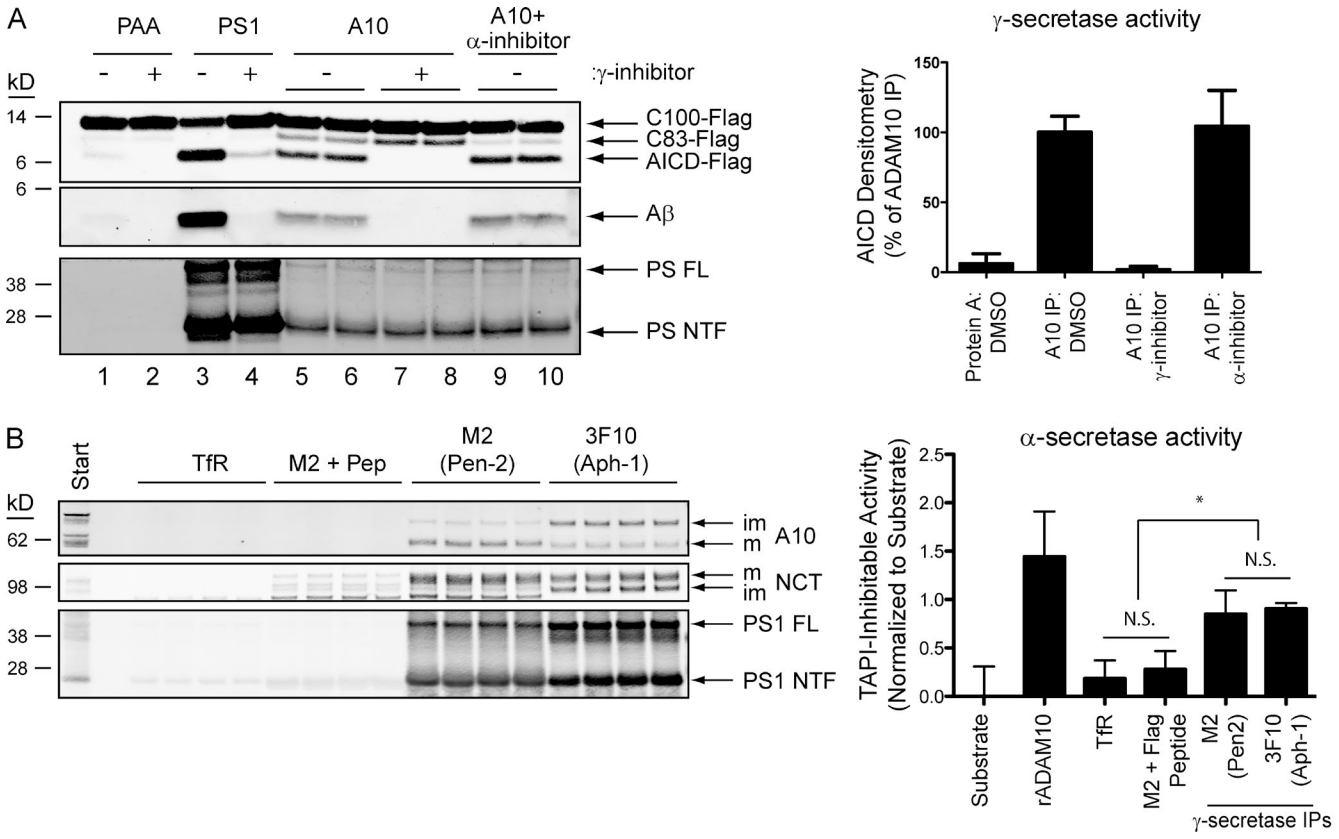

Figure 5. **The coimmunoprecipitated α–γ-complex contains both α- and γ-secretase proteolytic activities.** (A) S20 lysates were immunoprecipitated for A10, PS1, or just PAA. The immunoprecipitates were subjected to a γ-secretase activity assay (see Activity assays in Materials and methods) using a C100-Flag APP substrate. γ-Secretase activity was documented by generation of both AICD and Aβ via WB (left). The AICD generation was quantified (right). (B) S20 lysates were immunoprecipitated for γ-secretase using M2 (to Flag-Pen2) or 3F10 (to Aph-1-HA) and as controls TFR or M2 preabsorbed with Flag peptide. α-Secretase activity assays were performed on the resin using a fluorogenic peptide substrate (left) and quantified (right). A one-way ANOVA with Tukey's posttest for multiple comparisons was used. *, $P < 0.05$. $n = 6$. After the activity assays, the immunoprecipitates were eluted and blotted for coIP of A10, NCT, and PS1 NTF. Error bars indicate the SD. im, immature; m, mature.

acceptor (on A10), we observed a shortening of the Alexa Fluor 488 lifetime to 2,186 ± 91 ps, resulting in a fluorescence resonance energy transfer (FRET) efficiency of 8.4 ± 3.8% and thus demonstrating close atomic proximity (<10 nm) between some PS1 and A10 molecules and supporting our other extensive morphological and biochemical evidence that the two proteins can interact.

γ-Secretase inhibition, but not modulation, induces a feedback mechanism that activates A10-mediated α-secretase processing and concomitantly reduces β-secretase processing

We next asked whether our identification of endogenous, proteolytically active α–γ-secretase complexes in normal cells and brain might be associated with a functional consequence of inhibiting γ-secretase on the processing of substrates by α-secretase. Upon treating 7W CHO cells, which express human APP but only endogenous α- and γ-secretases, with the γ inhibitor DAPT, we observed a robust increase in APPs-α levels in their conditioned media (CM; Fig. S3 A). This increase in APPs-α was presumably the result of an α-secretase, as a general metalloprotease inhibitor (TAPI-I) ablated the increase (Fig. S3 A). To determine which α-secretase was responsible for this apparent feedback mechanism, siRNAs targeting ADAM9, A10, or TACE were transfected into the 7W cells. Knockdown of endogenous A10 largely prevented the increase in APPs-α seen upon γ inhibition (Fig. S3 B, quantified in C), whereas knockdown of endogenous ADAM9 or TACE did not, indicating that A10 was the responsible α-secretase.

Next, we sought to confirm these results in cells that also do not overexpress APP. When untransfected human M17D cells were treated with DAPT, γ-secretase was inhibited (robust increase in APP CTFs) and the APPs-α in the CM was significantly elevated (Fig. S3, D and E); this effect occurred without any significant change in the levels of endogenous full-length APP and mature and immature A10 and PS1 (Fig. S3 D). In these experiments, we observed a concomitant decrease in APPs-β levels, thereby elevating the ratio of APPs-α/APPs-β significantly after DAPT treatment (Fig. S3 E).

To rigorously confirm this intriguing finding, we tested a range of additional γ-secretase inhibitors, including some that have been studied in human (AD) trials. γ-30 cells were treated with DAPT, Avagacestat (BMS-708136), Begacestat (GSI-953), BMS-299897, Semagacestat (Lilly L450139), and three different Notch-sparing γ-secretase inhibitors synthesized in our center (AD1112, AD1113, and AD1138; Fig. 7 A). We assayed the APPs' secretion into the CM by WB and by ELI SA. Almost all the γ inhibitors robustly inhibited γ-secretase activity (as shown by a substantial increase in APP CTF levels), and they simultaneously enhanced the generation of APPs-α

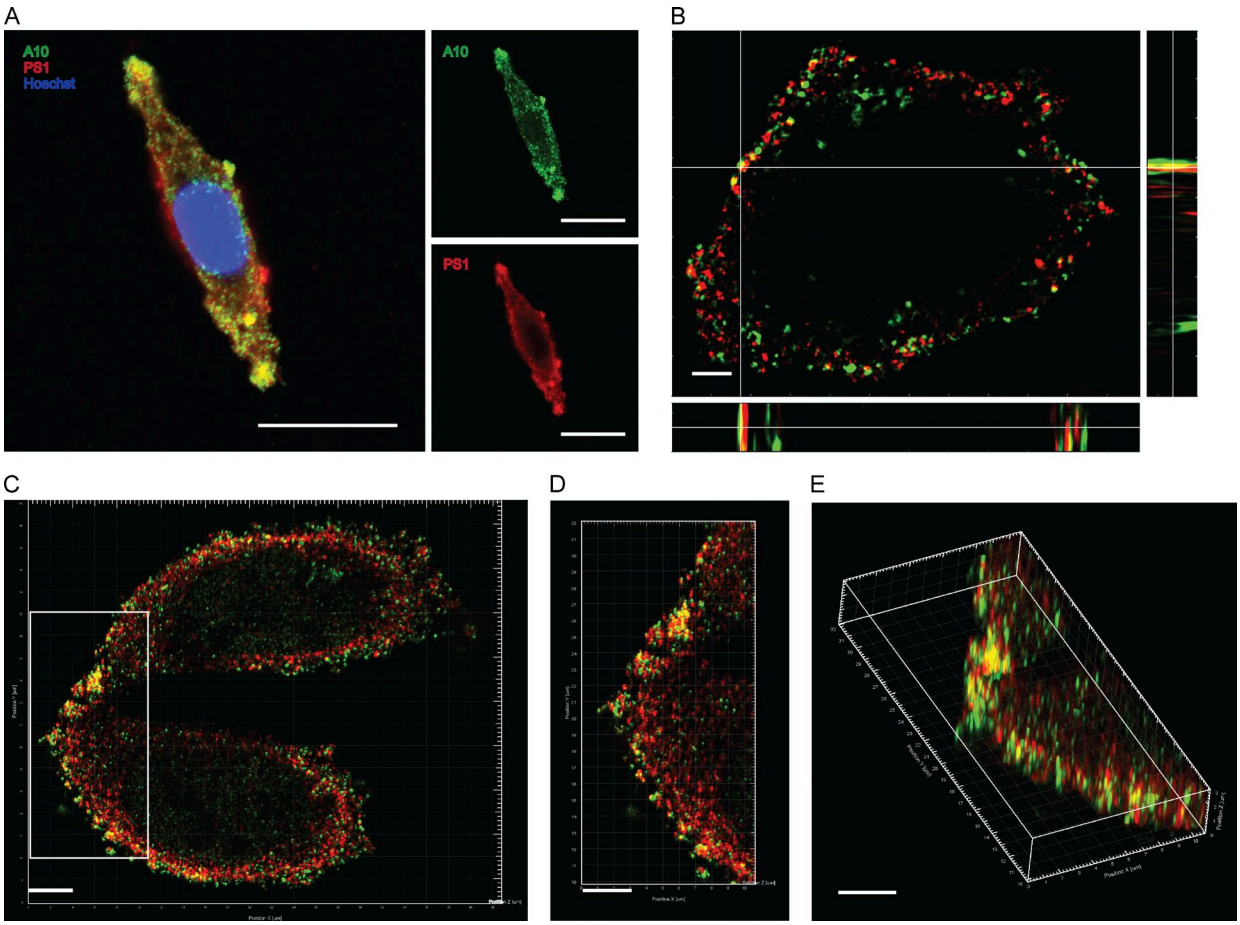

Figure 6. **Confocal microscopy and SIM of A10 and γ-secretase in 7W cells.** (A) A 1-µm optical section of 7W cells stained for A10 (green), PS1 (red), and Hoechst by confocal microscopy (left). Individual channel image for A10 (green, top right) and PS1 (red, bottom right). (B) Orthogonal view of SIM image showing colocalization (yellow) of some A10 (green) and PS1 (red) immunoreactive puncta in 7W cells. (C) Superresolution SIM images of A10 (green) and PS1 (red) immunoreactive puncta in 7W cells. (D) Magnified image of inset in C. (E) 3D-rendered image of D by Imaris processing. Bars: (A) 20 µm; (B) 2 µm; (C) 4 µm; (D and E) 3 µm.

(Fig. 7 A, quantified in B). Interestingly, Semagacestat in our hands did not robustly inhibit γ-secretase; in agreement, the resulting increase in APPs-α was much lower than with the other inhibitors. AD1113 produced no inhibition of γ-secretase and likewise did not result in increased APPs-α. When the levels of γ inhibition (i.e., degrees of increase in APP CTF levels) were plotted against the levels of APPs-α generation, we observed a correlation coefficient of 0.86 (Fig. 7 D), showing that the level of γ-secretase inhibition was highly correlated with the corresponding level of APPs-α secreted. When we assayed for APPs-β in the same CM by ELISA (Fig. 7 C), γ inhibition proportionately reduced APPs-β levels, suggesting that the increase in α processing is at the expense of β-secretase processing. We confirmed all of these inhibitor effects in γ-30 cells in our 7W cell line that expresses only endogenous levels of both α- and γ-secretase (unpublished data). Collectively, these data strongly suggest that there is a robust functional cross-regulation between γ-secretase activity and both α-secretase and β-secretase activity, further supporting our overall hypothesis that the secretases play interconnected physical and functional roles in the physiological processing of substrates.

To determine whether a γ-secretase modulator also affected APPs-α or -β secretion similar to γ inhibitors, we treated 7W cells with the canonical and well-characterized γ-secretase modulator, sulindac sulfide. As expected, treatment with 50-µM sulindac sulfide significantly reduced the Aβ42/40 ratio to 7%, from 10% (Fig. S4 B); however, this treatment did not affect the levels of APPs-α secretion by WB (Fig. S4 A) nor alter the APPs-α/-β ratio by ELISA (Fig. S4 C).

We next asked whether AD-causing mutations in PS1 could themselves alter the amount of APP shedding by α- or β-secretase. HEK293 cells stably expressing WT APP plus either WT PS1 or familial AD (FAD)–causing PS1 mutations (M146L, L392V, or Y115H; Citron et al., 1997) showed that each mutation significantly increased the Aβ42/40 ratio in the CM well above the normal ~0.15 ratio of WT cells as expected (Fig. S4 D). Quantifying the levels of APPs-α and APPs-β by ELISA revealed no significant difference between WT PS1 and any of the PS1 mutant lines (Fig. S4 E).

γ-Secretase inhibition does not alter the association between A10 and γ-secretase but instead leads to increased cell surface presentation of APP and BACE1

To further explore the mechanistic basis of the positive feedback on the α-secretase processing of substrate by inhibiting γ-secretase, we asked whether γ inhibition increased the physical association between γ-secretase and A10. S20 cells were

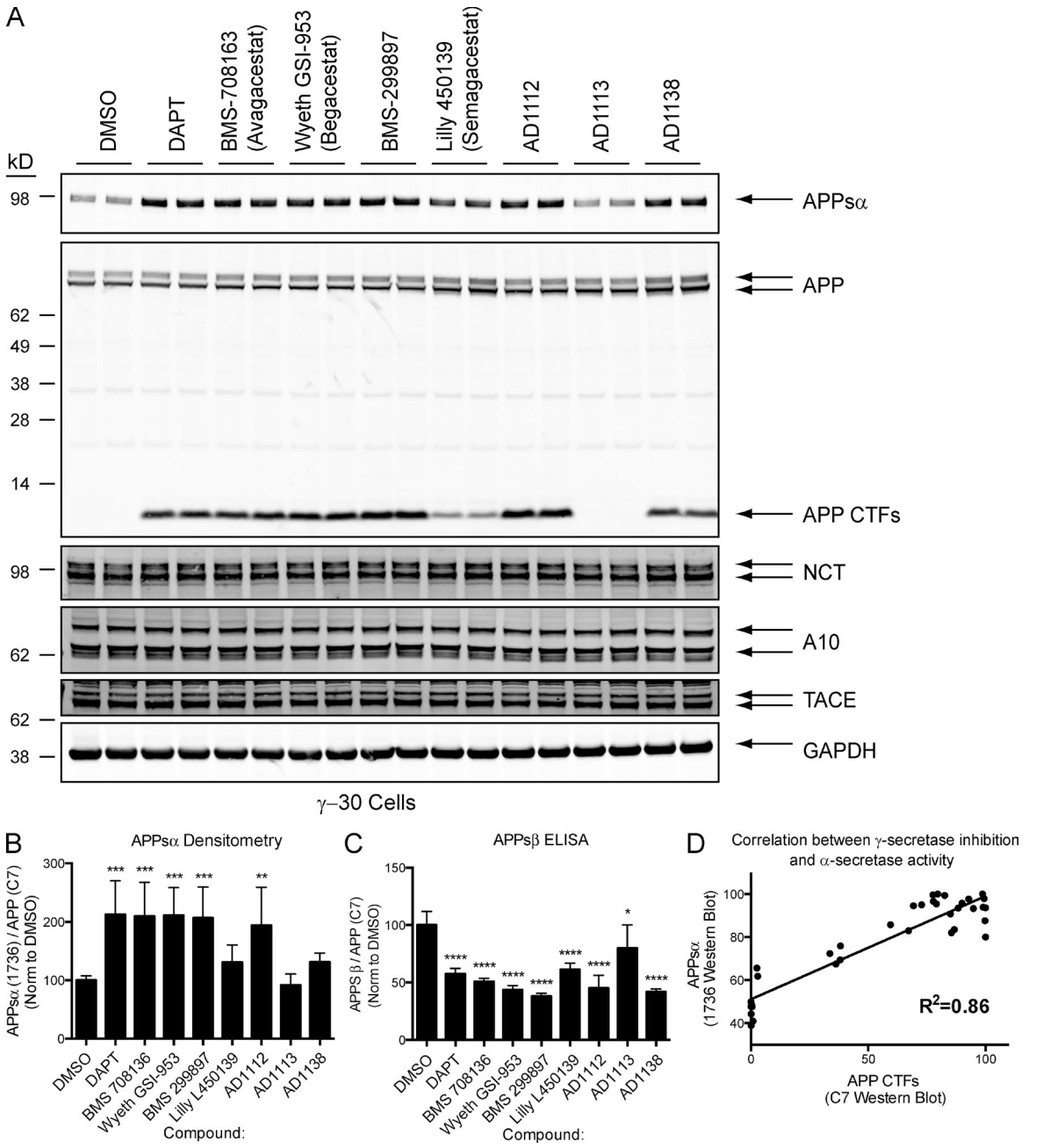

Figure 7. **Multiple structurally diverse γ-secretase inhibitors regulate processing by α- and β-secretase.** (A) γ-30 cells were treated with various γ inhibitors for APP, and the CM and lysates were analyzed for the indicated proteins. (B) Western blot quantification of APPs-α was performed on CM samples from A, normalized to total APP levels in the lysate, and then normalized to DMSO-treated control samples. A one-way ANOVA with Dunnett's posttest using DMSO as the control was performed. *n* = 6. (C) APPs-β ELISA was performed and quantified. All samples were equalized for APP levels, normalized to the DMSO-alone sample, and then analyzed by the same statistical test as in B. *n* = 4. (D) Levels of APP CTFs in lysates were plotted against APPs-α levels in CM (from Fig. 8 A) and fitted with a linear regression line. *n* = 36 from two independent experiments. *, P < 0.05; **, P < 0.01; ***, P < 0.001; ****, P < 0.0001.

treated with DAPT, immunoprecipitated for γ-secretase with M2 resin (to Flag-Pen2), and blotted for A10 (Fig. S5 A). Although DAPT treatment again increased the levels of APPs-α secretion (Fig. S5 B), it did not change the association between mature A10 and mature γ-secretase.

As yet another approach to examine the mechanism of the γ→α feedback, we asked whether the cell surface presentations of A10, γ-secretase, BACE1, or the APP substrate were altered by γ inhibition. 7W cells were treated with DAPT or DMSO, and 24 h later they were treated with a non–cell permeant biotinylation reagent, lysed, and pulled down with streptavidin to enrich for cell surface proteins (Fig. 8 A). γ inhibition did not alter the cell surface levels of mature γ-secretase (i.e., PS1 CTF and mature NCT), mature A10 (immature A10 was not biotinylated as expected, providing an excellent control for the specificity of our intact-cell surface labeling), or the canonical recycling protein TFR (Fig. 8 A), whereas it again substantially increased APPs-α levels in the medium (Fig. 8 B). In contrast, the levels of APP at the cell surface were elevated to 184 ± 45% of the control (DMSO) by the

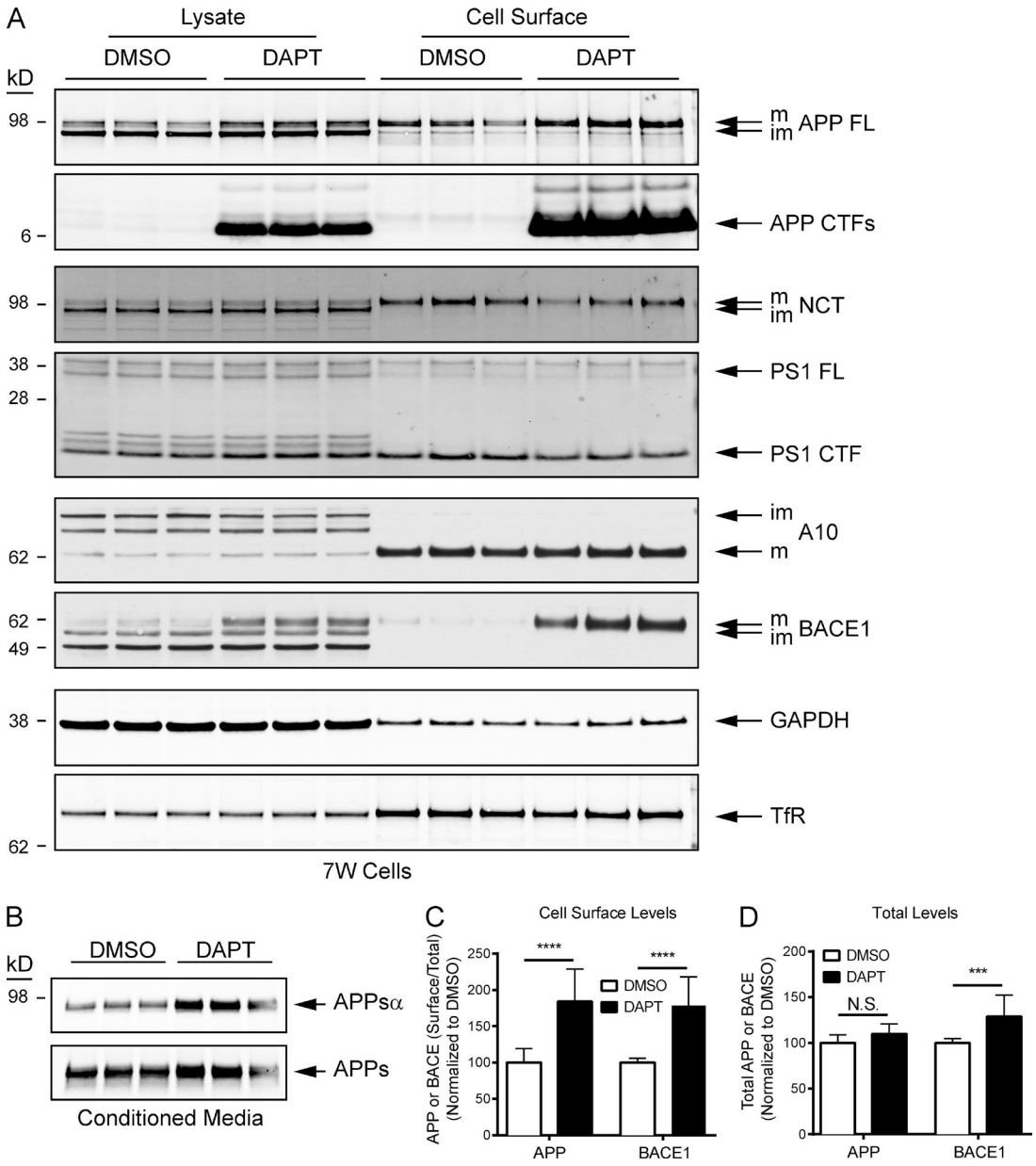

Figure 8. **Inhibition of γ-secretase activity increases the cell surface presentation of APP and BACE1.** (A) Top: 7W cells were treated with DAPT, and cell surface proteins were labeled with a non–cell permeable biotinylation reagent. Lysates from the biotinylated cells were pulled down with streptavidin. Whole lysates (left) and cell surface proteins (right) were probed for the indicated proteins. (B) CM from A were analyzed for APPs-α and total APPs by WB. (C) Surface levels of APP and BACE were quantitated from A and normalized to total APP or BACE levels in the lysate, respectively. A two-way ANOVA with a Sidak's posttest was performed. ****, $P < 0.0001$. $n = 8$. (D) Total lysate levels of APP and BACE were quantitated from A and normalized to total protein concentration. A two-way ANOVA with a Sidak's posttest was performed. ***, $P < 0.001$. $n = 8$. im, immature; m, mature.

DAPT treatment (Fig. 8 A, quantified in C). This consistent finding could explain why α-secretase cleavage of APP was increased at the expense of β-secretase, because α-secretases have been shown to cleave substrates (including APP) preferentially at the cell surface (Koo et al., 1996; Gutwein et al., 2003). Interestingly, we found that levels of BACE1 at the cell surface were also elevated to 179 ± 40% of the DMSO control by γ inhibition (Fig. 8 A, quantified in C). Because BACE1 is an aspartyl protease and works optimally in acidic pH of early and late endosomes, BACE1 processing of APP should be decreased by this enhancement of BACE1 levels at the plasma membrane (i.e., neutral pH), and that is just what we had documented (Fig. 7 C). γ inhibition did not significantly affect the total levels of APP in the lysate but did slightly increase BACE1 levels to 129 ± 23% of DMSO-treated control (Fig. 8 A, quantified in D). This stabilization of BACE1, however, cannot explain the much larger increase in the surface localization of BACE1. Collectively, these mechanistic experiments suggest that acute pharmacological inhibition of endogenous γ-secretase increases the total levels of mature BACE1 and particularly increases the levels of mature APP and BACE1 at the cell surface, thus enhancing APPs-α shedding at the expense of APPs-β without altering the surface levels of A10 and γ-secretase.

Select tetraspanin (TSPAN) proteins help mediate the stability and function of the α–γ-secretase complex

The TSPAN web has been extensively implicated in the stability and activity of A10 and separately for γ-secretase (Arduise et al., 2008; Wakabayashi et al., 2009; Xu et al., 2009; Dunn et al., 2010; Dornier et al., 2012; Haining et al., 2012; Prox et al., 2012). Specifically, TSPAN12 and the TSPAN C8 family (TSPAN5, 10, 14, 15, 17, and 33) have been reported to be important for A10 stability, localization, and activity. We sought to determine whether these candidate TSPANs may play a role in the α–γ-complex we have identified. siRNA-mediated knockdown of TSPAN5 and 14, or else of TSPAN12 and 17 (T10, T15, and T33 are not expressed in our CHO-based cells; unpublished data), were each able to reduce APPs-α secretion (Fig. 9 A, bottom). TSPAN12 and 17 knockdown did not affect A10 levels or maturation, whereas TSPAN5 and 14 knockdown decreased A10 maturation and increased the levels of immature A10 (Fig. 9 A). Next, we sought to determine whether knocking down these candidate TSPANs would affect the A10–γ-secretase interaction. S20 cells were transfected with siRNAs targeting TSPAN5 + 14, TSPAN12 + 17, or all four and were then immunoprecipitated for γ-secretase (via Pen-2) and probed for the coimmunoprecipitate of A10 (Fig. 9 B). We saw that knockdown of these two pairs of TSPANs consistently reduced the level of coIP of mature A10. Although there was less coIP of A10 upon TSPAN5 + 14 knockdown, there were also reduced levels of mature A10 in the total lysate, making it difficult to conclude whether the observed reduction in coIP from this pair was the result of a decrease in the association of A10 with γ-secretase or just a result of the reduced levels of A10 protein. In contrast, knockdown of TSPAN12 + 17 did not reduce the total cellular levels of mature A10 but still reduced the degree of coIP with γ-secretase, suggesting that this pair of TSPANs in particular is important for α–γ-complex formation and/or stability.

In light of this intriguing result, we sought to determine whether the TSPANs that help mediate α–γ-complex assembly are also involved in the γ→α feedback mechanism. 7W cells were first transfected with TSPAN12 + 17 siRNAs as in Fig. 9 B and were then treated with increasing doses of DAPT (Fig. 9 C), and their CM were analyzed for the APPs-α/APPs-β ratio by ELISA (Fig. 9 D). Treatment with increasing doses of DAPT resulted in an increase in APP CTFs, demonstrating a dose-dependent inhibition of γ-secretase as expected (Fig. 9 C). In control samples (no TSPAN knockdown), the APPs-α/-β ratio at the maximal dose of DAPT tested (1 µM) resulted in a 4.8-fold increase above the DMSO-treated control. Knockdown of TSP AN12 + 17 reduced baseline APPs-α levels as before (Fig. 9 C, see lowest doses of DAPT used), but there was a reduction of the APPs-α/-β ratio at the maximal dose of DAPT (1 µM) to just 3.8-fold above the DMSO control. Likewise, the differences in the dose–response curves were significant at the 0.033-µM and 0.1-µM DAPT concentrations (Fig. 9 D). In other words, DAPT at a particular dose was less effective in raising the APPs-α/-β ratio after a TSPAN12 + 17 knockdown that decreases the association of α- and γ-secretases in cells. The levels of A10 and PS1 were not affected by both TSPAN12 + 17 knockdown and DAPT (Fig. 9 C). Together, these integrative data suggest that manipulating TSPAN12 and 17 alters the γ→α-/β-secretase feedback mechanism when it simultaneously destabilizes the A10–γ-secretase complex.

Coordinate processing by complexes of a sheddase and an intramembrane protease may represent a general model extendable to the β- and γ-secretases

Finally, we asked whether the new cell biological model of RIP described thus far could be generalized to β-secretase. To this end, we probed whether β-secretase also interacts with γ-secretase. Microsomes from WT mouse brains, which have high endogenous expression of BACE1 (β-secretase), were immunoprecipitated for endogenous PS1 CTF and blotted for the coIP of BACE1 (Fig. 10 A). IP of PS1 CTF brought down endogenous BACE1, indicating that β-secretase can also interact with γ-secretase. Importantly, this finding was also observed in the reverse direction, in that several BACE1 antibodies (Fig. 10 B) were each able to coimmunoprecipitate endogenous PS1 CTF, whereas no significant coIP with TFR occurred. The results demonstrate that endogenous β-secretase, like α-secretase, can interact with endogenous γ-secretase in a multisecretase complex.

We examined whether α- and β-secretase interacted with γ-secretase in the same complex or in distinct complexes. To this end, we performed IPs for A10 (Fig. 10 C) or BACE1 (Fig. 10 D) and blotted for the coIP of BACE1 or A10, respectively. IP of A10 or BACE1 did not bring down detectable amounts of the other sheddase. This consistent result indicates that we were unable to detect A10 and BACE1 interacting together in a super complex and that they may each form separate complexes with γ-secretase.

Discussion

Here, we provide multiple lines of experimental evidence that the processing of membrane proteins by the α- and γ-secretases can occur within a single, multiprotease complex. We establish that the principal α-secretase, A10, associates with γ-secretase in a larger functional complex. Further, we demonstrate that this is extendable to β- and γ-secretases, as BACE1 was shown to associate endogenously with γ-secretase. It is possible that other intramembrane proteases such as S2P and signal peptide peptidase may also associate with their respective sheddases. Indeed, our preliminary data indicate that S2P can associate with S1P (unpublished data), suggesting that this new model may be relevant to the biological mechanism of RIP by other intramembrane proteases.

A10 and γ-secretase interact at both overexpressed and endogenous levels and at a site—the plasma membrane—where each has been well documented to be active. We also observed an interaction between TACE and γ-secretase; indeed, as an important control for specificity, this interaction was not seen in neural cells or mouse brain, where abundant immature but little mature TACE is present. Thus, the precise composition of the heteromeric α–γ-secretase complexes we describe may be cell type dependent. By SEC, mature A10 fractionated with mature γ-secretase in an HMW complex, and the two endogenous secretases could be coimmunoprecipitated from such fractions of normal mouse brain. Furthermore, A10 and γ-secretase co-migrated in an HMW complex of ∼440 kD by BN-PAGE.

Importantly, we found that the α–γ-complex is functional, as both α- and γ-secretase proteolytic activities were recovered by coimmunoprecipitating either secretase. In addition to physical and functional interactions, we observed an unexpected and robust increase in the α-secretase shedding of APP upon γ inhibition. This quantitative and highly significant correlation ($r = -0.86$) was documented with multiple γ inhibitors, including some used

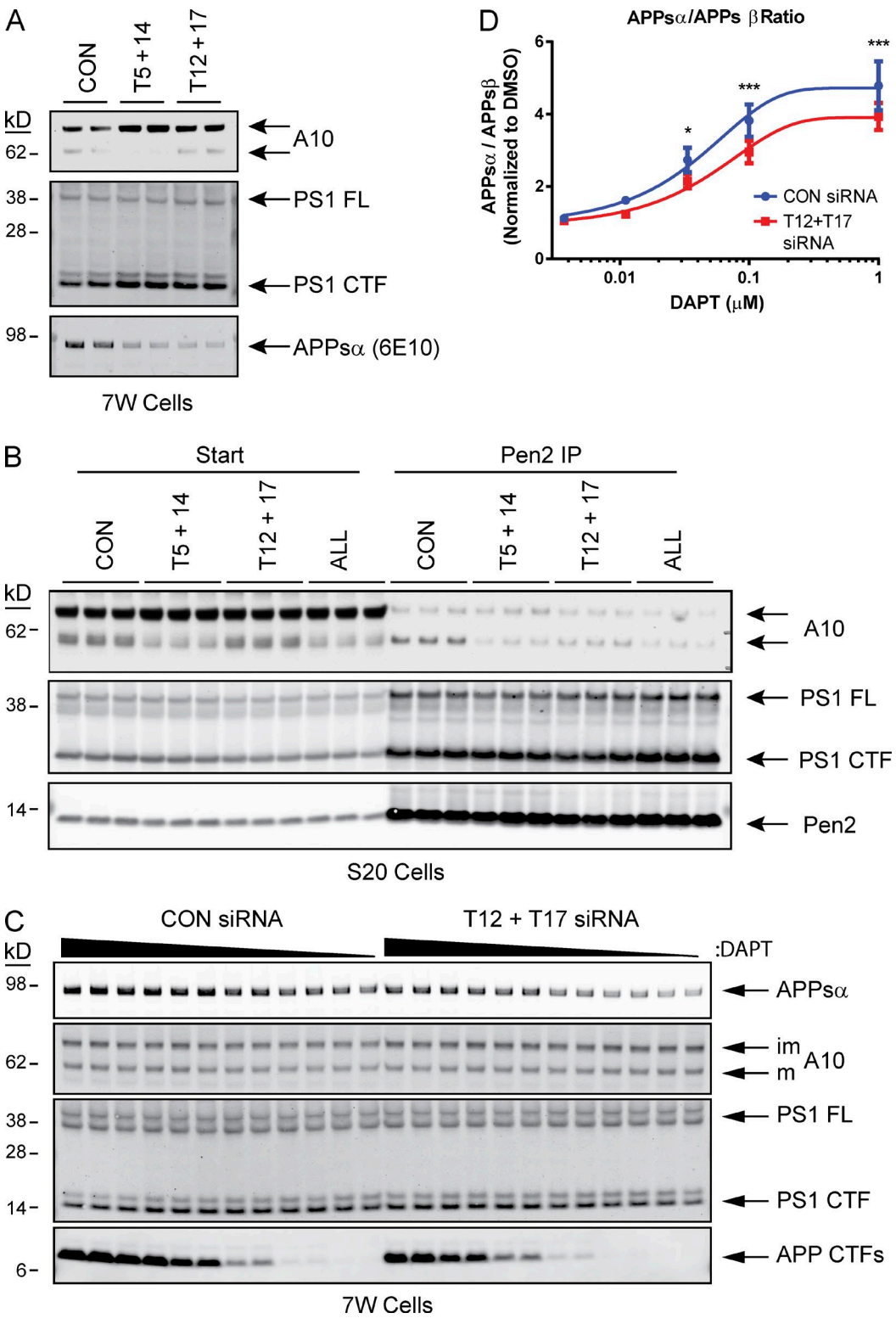

Figure 9. **TSPAN12 and 17 are required for A10 and γ-secretase association and contribute to the α–β-secretase activity regulation by γ inhibition.** (A) 7W cells were transfected with siRNA targeting TSPAN5 + 14, TSPAN12 + 17, or the control. CM were analyzed for APPs-α and lysates for A10 and PS1. (B) S20 cells were transfected with siRNA as in A, and the resultant lysates were immunoprecipitated for γ-secretase by pull-down of Flag–Pen-2 (via an M2 resin). The resulting immunoprecipitates were probed for the coIP of A10 and other γ components. (C) 7W cells were transfected with control siRNA or siRNA targeting both TSPAN12 and 17 and treated in duplicate with increasing amounts of DAPT (3 nM–1 μM). The resulting CM was probed for APPs-α and lysates for A10, PS1, and APP CTFs. (D) CM from C was analyzed by an MSD ELISA for APPs-α and APPs-β. Data are represented as a ratio of APPs-α/APPs-β. A two-way ANOVA with a Sidak's posttest was performed. *, $P < 0.05$; ***, $P < 0.001$. $n = 6$. CON, control; im, immature; m, mature.

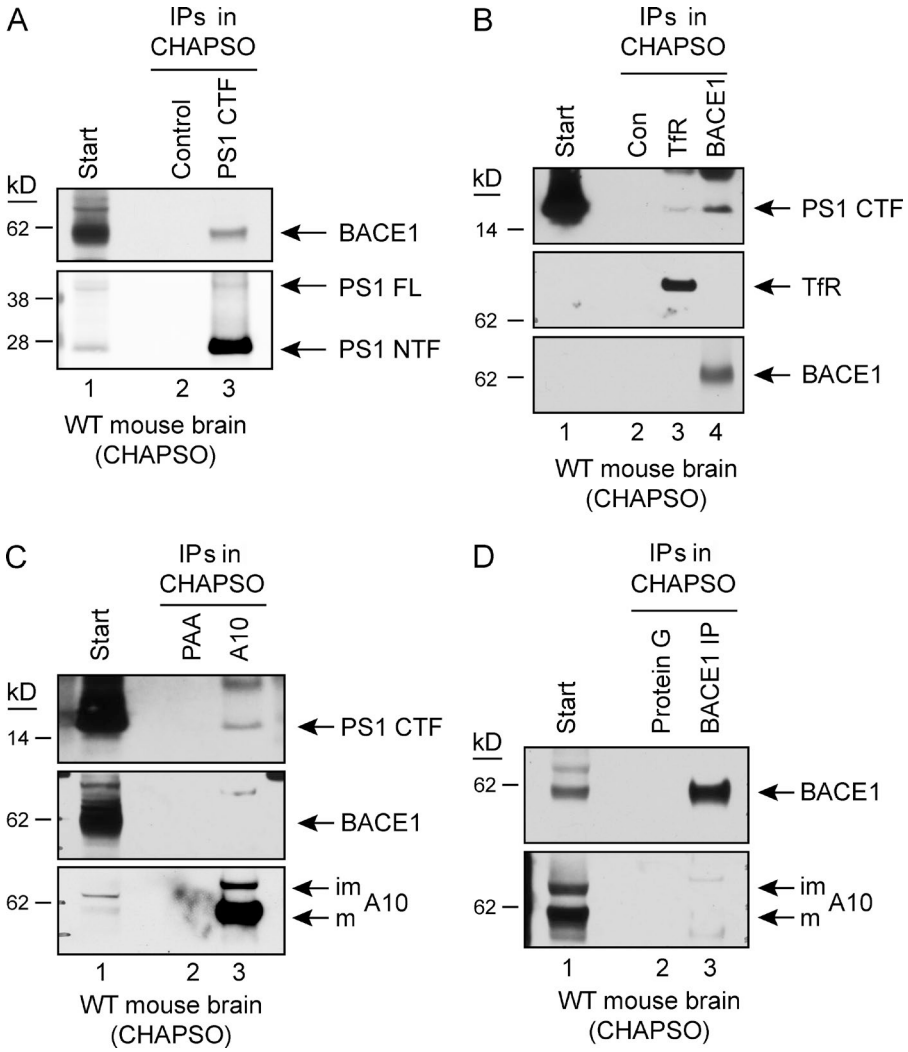

Figure 10. **BACE1 also interacts with γ-secretase but not with A10.** (A) CHAPSO-solubilized mouse brain microsomes were immunoprecipitated for PS1 CTF or using control resin. Immunoprecipitates were probed for PS1 NTF and for the coIP of BACE1. (B) Mouse brain microsomes solubilized in 1% CHAPSO were immunoprecipitated for BACE1 or TFR and probed for the coIP of PS1 CTF. (C and D) Mouse brain microsomes were immunoprecipitated for A10 (C) or BACE1 (D) and probed for the coIP of BACE1 or A10, respectively. Con, control; im, immature; m, mature.

in AD clinical trials: Begacestat, Avagacestat, and Semagacestat. The highly consistent increase in α-secretase processing of APP upon γ inhibition occurred at the expense of β-secretase processing. Mechanistically, the stimulatory effect of γ inhibition on APP shedding is a result, at least in part, of substrate trafficking, as γ inhibition enhanced levels of APP (and BACE1) at the cell surface. Both γ modulators (which do not abrogate γ-secretase cleavage per se) and FAD mutations in PS1 did not consistently alter α-secretase activity.

Collectively, our findings have implications for the fundamental biology of the secretases in cells. We observed specific interactions of A10 and of BACE1 with γ-secretase but could not coimmunoprecipitate the three proteases together in a supercomplex. It thus becomes important to determine whether BACE1, A10, and TACE each occur in distinct complexes with γ-secretase, analogous to how PS1 and PS2 as well as the three principal isoforms of Aph-1 can each form distinct complexes with the other proteins of γ-secretase (De Strooper, 2003; Hébert et al., 2004; Shirotani et al., 2004). We hypothesize that the complexes we have identified may be cell type dependent, explaining why in some cells, certain coIPs were not observed (e.g., in neural M17D cells, TACE did not coIP with γ-secretase, probably because TACE exists exclusively in its immature form). This hypothesis may be relevant to the long and growing list of γ-secretase substrates, as there may exist several different cellular complexes composed of different variations of sheddases and γ-secretases that are each responsible for processing a subset of substrates for reasons of substrate structure or subcellular localization. Multiple γ-complexes comprising various PS and Aph-1 isoforms have been identified and reconstituted (Hébert et al., 2004; Shirotani et al., 2004). Whether these γ-complexes interact differentially with the various α- and β-secretases now becomes important to answer. Despite our negative results to date, we cannot exclude that both BACE1 and A10 can sometimes form a single large complex with γ-secretase in certain subcellular compartments. This could explain why α- and β-secretases sometimes compete with each other for processing of substrates. Also, it has been shown that α-secretase (A10) may efficiently cleave C99 under endogenous conditions (Kuhn et al., 2010), and we found evidence of such processing in our A10 coIP activity assays (Fig. 5 A). But under endogenous conditions, we have so far not identified an interaction between BACE1 and A10.

Although several screens have been performed to identify novel γ interactors, none to our knowledge has identified A10 or BACE1 (Zhou et al., 2005; Wakabayashi et al., 2009; Hur et al., 2012; Teranishi et al., 2012). The degree of coIP between A10 or BACE1 and γ-secretase in our study was not as high as the coIP of the four canonical members of the γ-complex, which could explain the prior lack of identification of α-secretase as a γ interactor.

One probable explanation that our mechanistic data support is that the α–γ- and β–γ-secretase interactions are indirect and occur within a larger multiprotein complex to finely regulate substrate processing. Although we used multiple methods (coIP, biochemical cofractionation, native PAGE, superresolution microscopy by SIM, and FLIM) and examined multiple cell/tissue sources to obtain clear evidence that an α–γ interaction does occur endogenously, we also obtained evidence that this interaction is indirect, i.e., mediated by other scaffolding partners like the TSPAN. Specifically, we demonstrate here that TSPAN5 and 14 can affect both the maturation and activity of A10 and that TSPAN12 and 17 affect A10 activity without detectably altering A10 maturation; however, both sets of TSPANs were shown to mediate, in part, the association between A10 and γ-secretase.

A10 has previously been shown to be a substrate of RIP processing by γ-secretase (Tousseyn et al., 2009). We provide several lines of evidence here that the interaction between A10 and γ-secretase that we describe is not simply that of a substrate (A10) and a protease (γ-secretase) but represents a functional, biologically relevant complex. First, under endogenous expression levels, predominantly the mature forms of the secretases interact with each other. This was particularly well seen in normal mouse brain tissue, where principally mature A10 was found to interact with mature γ-secretase (Figs. 2 and 3). Second, we document an interaction at the plasma membrane, where both mature secretases are known to reside and to process numerous substrates (Fig. 2 D). Third, we observed that the complex, upon coIP, contains both α- and γ-secretase cleavage activities (Fig. 5). Fourth, we observed what appears to be sequential processing by α- and γ-secretase of a canonical APP substrate (Fig. 5 A). In the presence of the immunoisolated α–γ-complex, a fragment corresponding to C83 was generated from C100 (i.e., C99 with a translation-initiating methionine), and this C83 generation was inhibited by TAPI-I, consistent with it arising from α processing. Moreover, this C83 fragment was stabilized by a γ inhibitor, suggesting that it is further processed by γ-secretase to p3 and AICD, as expected. These experimental results are entirely consistent with sequential α- and γ-secretase processing of C100. Lastly, we observed a stronger level of interaction between A10 and γ-secretase than APP and γ-secretase. In our γ-30 cells, which have overexpressed APP and high levels of γ-secretase, we saw a more robust coIP of γ-secretase with endogenous A10 than with the overexpressed APP (Fig. 2 A; compare the enrichments of APP vs. A10 and vs. TACE). Together, these data support our hypothesis that A10 and γ-secretase reside in a higher molecular weight complex that is capable of accepting full-length substrates for sequential processing.

Beyond the physical interaction between the secretases, we provide evidence that the cleavages mediated by these ubiquitous proteases are much more functionally interconnected than previously believed. Our finding that pharmacological inhibition of γ-secretase increased α-secretase processing of APP (Figs. 7 and S3) could explain a report that prolonged treatment of humans with Semagacestat modestly elevated levels of APPs-α in the CSF and also significantly increased an α-secretase product of C99, Aβ16 (Portelius et al., 2010). Moreover, a recent publication demonstrated that a FAD mutation in the γ cleavage region of APP resulted in an increase in APPs-β secretion, and this increase was prevented by a γ inhibitor (Muratore et al., 2014), consistent with our model of cross talk within a functionally interconnected secretase network. A practical outcome of our work here is that future studies examining the effects of γ-secretase inhibitors, including those in clinical trials for AD or cancer, should closely examine their effects on α- and β-secretase processing, which could lead to unwanted side effects. Furthermore, we establish that this feedback mechanism is dependent at least in part on the α–γ-complex, as weakening of this complex by selective knockdown of TSPAN12 and 17 simultaneously reduced the feedback of γ inhibition on α- and β-secretase processing of a canonical substrate.

Mechanistically, the enhancement of APP shedding by pharmacological γ inhibition is likely a result of the increase this caused in the cell surface presentation of mature APP, where A10 predominantly cleaves its substrates (whereas BACE1 predominantly cleaves substrates in acidic environments like recycling endosomes). This phenomenon has been previously suggested, in that cells expressing a catalytically inactive form of PS1 had enhanced retention of APP (and presumably many other substrates) at the cell surface (Kaether et al., 2002). We also observed an increase in BACE1 at the cell surface, but, not unexpectedly, we did not see an increase in β-secretase processing of APP. At least two factors could explain the latter finding. First, BACE1 is an aspartyl protease that cleaves optimally at pH 4.5 in vitro (Vassar et al., 1999). Thus, the neutral pH found at the cell surface is not optimal for BACE1 activity. Second, the increase in BACE1 on the plasma membrane is likely a result of the retention of mature BACE1 at the cell surface and not because of increased trafficking of BACE1 from the ER to the surface, as immature BACE1 remained unchanged. The BACE1 molecules that are prevented from being endocytosed into endosomes are thus retained in a compartment where they cannot efficiently process substrates. It is likely that these previously unrecognized trafficking effects arising from γ inhibition occur with other substrates besides the canonical γ substrate, APP.

In summary, our numerous biochemical and cell biological findings provide new directions for future research on the mechanism of RIP in health and disease: (a) the data on α–γ- versus β–γ-complexes suggest the occurrence of distinctly composed multisecretase complexes that may have specialized functions for processing some but not other substrates; (b) our inhibitor experiments uncover an unexpected and robust regulation of α-secretase activity by γ-secretase activity, a cross talk that was not anticipated but needs to be known to predict potential side effects of chronically inhibiting γ-secretase in cancer and AD; (c) in contrast to γ-secretase inhibitors, γ-secretase "modulators" do not trigger this cross-regulation, supporting their clear advantage for human therapy; (d) collectively, the extensive data herein support a new cell biological model of RIP in which the sheddase and the intramembrane protease reside together in a higher molecular weight complex mediated in part by select members of the TSPAN and capable of accepting full-length transmembrane substrates and processing them to their end products rapidly and efficiently.

Materials and methods

Reagents, cell culture, inhibitor treatments, and transfections

All siRNAs were obtained from the siGenome series (GE Healthcare) of siRNAs (Table 1). All constructs ordered were pools of four sequences per target.

DAPT was purchased from Sigma-Aldrich, whereas all other inhibitors were synthesized in-house and given to us by C. Augelli-Szafran (Brigham and Women's Hospital, Boston, MA). Sulindac sulfide was

purchased from Sigma-Aldrich. Our 7W, PS70, γ-30, and S20 CHO cell lines were cultured as previously described (Kimberly et al., 2003; Cacquevel et al., 2008). In general, cells were maintained in DMEM plus 10% FBS, 2-mM L-glutamine, 100 µg/ml streptomycin, and 100 U/ml penicillin, plus the appropriate selection antibiotic for each line. For inhibitor treatments, cells were conditioned for 4–16 h in Opti-MEM media (Gibco) with inhibitors at the following concentrations: 500-nM DAPT, 25-M TAPI-I, 15-nM BMS-708163 (Avagacestat), 150-nM Wyeth GSI-953 (Begacestat), 75-nM BMS-299897, 200-nM Lilly 450139 (Semagacestat), 350-nM AD1112, 30-nM AD1113, and 50-nM AD1138. For transient transfections, Lipofectamine 2000 (Invitrogen), Fugene 6, or Fugene HD (Roche) were used to transfect cDNAs into cells according to the manufacturer's standard protocol. Cells were harvested 24 h after transfection. For siRNA transfections, Lipofectamine RNAiMAX (Invitrogen) was used to transfect 50-nM siRNA into cells. Cells were harvested 48 h after transfection.

Sample preparation and IP

Whole cell lysates and microsomes were prepared as previously described (Chen et al., 2010). In brief, 10-cm culture plates were first washed with PBS and then lysed in 1 ml of 50-mM Hepes buffer + 150-mM NaCl containing either 1% CHAPSO, 1% digitonin, 0.25% DDM, or 1% NP-40, as stated. In some cases, 10-mM 1,10-phenanthroline was included in the lysis buffer. The lysates were then incubated on ice for 30 min and spun at 14,000 rpm on a tabletop microfuge to pellet insoluble material. For microsome preparations, cells were first Dounce homogenized with a tight pestle in TBS containing no detergent, followed by passage through a 27.5-gauge needle four times. Samples were then centrifuged at 1,000 *g* followed by a 100,000 *g* ultracentrifuge spin to pellet microsomes, which were solubilized in 50-mM Hepes buffer + 150-mM NaCl containing 1% of the detergent mentioned for 60 min, followed by another 100,000 *g* spin. Protein concentrations were determined for both lysates and microsomes by a bicinchoninic acid protein assay (Thermo Fisher Scientific), and all samples were normalized for equal concentration before experiments.

For immunoprecipitates, 0.8–1.5 mg of cell lysates or microsomes in 0.8–1.0-ml volumes of lysis buffer were precleared with protein A or G agarose for 90 min before IP. The immunoprecipitates were incubated overnight at 4°C and then washed three times in lysis buffer. The immunoprecipitated proteins were then eluted in SDS sample buffer. For the IP of tagged proteins, we used 3F10 resin (rat; Roche), HA7 resin (mouse; Sigma-Aldrich), Myc resin (rabbit; Sigma-Aldrich), and M2 resin (mouse; Sigma-Aldrich) for Flag-tagged proteins and V5 resin (mouse; Sigma-Aldrich). For IP of all other proteins, protein A or protein G agarose were added with antibodies targeting the specific protein. For A10 IPs, we used antibody 422751 (rabbit; EMD Millipore), 19026 (rabbit; EMD Millipore), 124695 (rabbit; Abcam), or 73402 (mouse; Abcam). For TACE, we used the rabbit antibodies ab75609 or ab2501 (both from Abcam). Rabbit antibody X81 (Xia et al., 1997a), directed against the first 81 residues of PS1, was used to IP PS1 NTF. For PS1 CTF, MAB5232 (mouse; EMD Millipore) and mouse antibody 13A11 (gift from Elan, plc, South San Francisco, CA; directed against the loop region of PS1) were used. Antibody ab84036 (rabbit; Abcam) and a mouse monoclonal antibody from Invitrogen were used to IP TFR. BACE1 antibodies 195102, 195111 (both Calbiochem and both rabbit), AB5832 (rabbit; EMD Millipore), and MAB5308 (mouse; EMD Millipore) were used for IP. A commercial antibody (rabbit; Abcam) was used to IP NPR A.

For lysate-mixing experiments done as a negative control for our coIPs, the untransfected 7W cells were used as a source of γ-secretase–negative cells (as they do not overexpress Flag–Pen-2 or human PS1), and S20 cells were used as γ-secretase–positive cells (as they do overexpress all four γ-secretase components). For A10-negative and -positive cells, cells were transfected with either A10 siRNA (A10 negative) or control siRNA (A10 positive). The lysates were protein quantified and mixed at a 1:1 ratio, and then the mixture was immunoprecipitated with an M2 resin to the Flag tag on Pen-2 that is present only in the S20 cells.

Electrophoresis and WB

Samples were loaded onto 4–12% Bis-Tris gels using MES or MOPS running buffer (Invitrogen), transferred to nitrocellulose membranes, and probed for various proteins using standard WB. The resultant blots were detected with either an infrared imaging system (Odyssey; LI-COR Biosciences) or by ECL and exposure to film.

The antibodies used to detect specific antigens were Flag tag, M2 (mouse) and a rabbit polyclonal anti-Flag antibody (both from Sigma-Aldrich); Myc tag, 9E10 (mouse) and A14 (rabbit; SCBT); HA tag, 3F10 (rat; Roche); A10, 422751 (rabbit; EMD Millipore), ab19026 (rabbit; EMD Millipore), PC528 (rabbit; EMD Millipore), ab73402 (mouse; Abcam), and ab124695 (rabbit; Abcam); TACE, ab75609 (rabbit; Abcam), ab19027 (rabbit; EMD Millipore), AF2129 (goat; R&D Systems), and a rabbit C-terminal antibody provided by C. Blobel (Weill Cornell Medical College, New York, NY); APP, C7 (rabbit antibody targeting the last 20 amino acids in APP; Podlisny et al., 1991), 22C11 (mouse; EMD Millipore), 6E10 (mouse; Covance), 1736 (rabbit; Haass et al., 1992), and two mouse monoclonal antibodies generated in-house that target either the APP ectodomain or C terminus (4F2 and 3F3, respectively); Aβ, mouse monoclonal antibodies 2G3 and 21F12 that target the C-terminal of Aβ40 and 42, respectively (a gift from Elan, plc). For γ-secretase components, we used NCT, N1660 (rabbit; Sigma-Aldrich), and a monoclonal antibodie (BD); for PS1, we used 529591 (rabbit, EMD Millipore), MAB1563 (rat; EMD Millipore), MAB5232 (mouse; EMD Millipore), 13A11, and 4627 (rabbit antibody that targets the extreme C terminus of PS1; Podlisny et al., 1997); and for Aph-1, we used O2C2 (rabbit; Thermo Fisher Scientific). For TFR, two antibodies from Invitrogen (H68.4; mouse) and Abcam (ab84036; rabbit) were used.

Table 1. **Sequences of siRNA used to knock down respective targets**

Target	Sequence 1	Sequence 2	Sequence 3	Sequence 4
ADAM9	GCAAAGAGCUGUAUCAUGA	GAGAUUAACUAGAGAAAGA	GAACCAGACUGCUGUGAGA	GCAGAUCUCUUACGUCAUC
ADAM10	GAAGGAAGCUUUAGUCAUG	CCCAAAGUCUCUCAUAUUA	GCAGAGAGAUACAUUAAAG	GAAUUGCCCUGAUCAUGUU
ADAM17	GAAAGACACUUCAAUAUGG	UAUGGGAACUCUUGGAUUA	GGUAGCAGAUCAUCGAUUU	UGACCGAGUUGAUGACAUA
TSPAN5	GGAAUAACGUUUCUUGGAA	GCGAUGCGGUGUGCCAUUU	GAUGAUUGGAACCUAAAUA	CAUAGGCAUUGCAUUGCUA
TSPAN12	GGUCAGAUAUGGUUACUUU	GAACGUUACUCGUCAUCUU	GCGGUCAUCUUAACUUACU	CAUACGAGCAGGAGGUUAU
TSPAN14	CAGCUACAAUAUCGUCUUU	GAACCUCAUUGACUCCCUU	GAACAUCUGCCUGCUCAAG	GGGAAUUCUUCGAGAGCAA
TSPAN17	GAUCCGAGACCAACUUAAU	ACAACAAUGUCAAAGCCUA	GAAUACUGGUCUUGCUGUG	UGACAGAUCUGGGCGGUCU
CONTROL	UAGCGACUAAACACAUCAA	UAAGGCUAUGAAGAGAUAC	AUGUAUUGGCCUGUAUUAG	AUGAACGUGAAUUGCUCAA

GE Healthcare siGENOME is a pool of four individual siRNAs. Sequences 5′- to -3′ for the individual siRNAs are listed for each target.

BN-PAGE

Cells were lysed in 50-mM Hepes buffer + 150-mM NaCl containing 0.25% DDM detergent and incubated on ice for an hour. Lysates were first spun at 1,000 *g* for 5 min to pellet nuclei and large cellular debris, and this was followed by a 100,000 *g* spin for 60 min. DDM-soluble lysates along with NativeMark protein standard (Invitrogen) were loaded onto a 4–16% Bis-Tris NativePAGE gel (Invitrogen) according to the manufacturer's specifications. Gels were transferred to a polyvinylidene fluoride membrane and probed for the indicated proteins by WB.

Surface biotinylation

S20 cells were washed three times with PBS and then treated with sulfo-NHS-SS-biotin at 0.5–1.0 mg/ml for 30 min at room temperature or at 4°C if stated. Reactions were quenched with 1-M Tris (50-mM final concentration) for 5 min and washed three times with TBS or PBS. Cells were lysed and immunoprecipitated for Aph-1 (HA7) or Pen-2 (M2) or alternatively, pulled down with streptavidin agarose as described and eluted with 1% SDS or sample buffer. Eluates from Aph-1 or Pen-2 immunoprecipitates were diluted 1:10 (final SDS concentration of 0.1%) and pulled down with streptavidin agarose (Sigma-Aldrich) overnight at 4°C. Pull-downs were washed, eluted with SDS sample buffer, and Western blotted.

SEC

Microsomes isolated from normal mouse brains or S20 cells were solubilized in 1% CHAPSO (250 µl of total volume), injected onto a Superose 6 10/300 column (24-ml-bed volume), and run on an fast protein liquid chromatography system (AKTA; GE Healthcare) in 50-mM Hepes buffer + 150-mM NaCl with 0.25% CHAPSO. 500-µl fractions were collected, concentrated, and analyzed by SDS-PAGE. In some experiments, certain SEC fractions were pooled and concentrated before IP for A10, NCT, or Aph-1.

Activity assays

For γ-secretase activity assays, a C100-Flag substrate was used (Esler et al., 2002). In brief, all reactions were performed on resin in Hepes buffer with 0.25% CHAPSO supplemented with 0.25 mg/ml phosphatidylethanolamine, 1 mg/ml phosphatidylcholine, and 0.065 mg/ml cholesterol. Reactions were incubated overnight at 37°C and terminated with SDS. Samples were then analyzed by WB or ELISA for Aβ or AICD as a measure of γ activity. The addition of γ inhibitors was used to determine γ-secretase–specific activity.

For α-secretase activity assays, we used a fluorogenic peptide substrate (based on the sequence of pro-TNF) that is unquenched when cleaved (ES003; R&D Systems). Substrate was used at a concentration of 10 µM in 25-mM Tris, pH 8.0, 2.5-µM ZnCl, 0.25% CHAPSO, and 0.005% Brij 35 in a total volume of 150 µl and was incubated for 4 h at 37°C. Reactions were stopped by adding EDTA and read on a florigenic plate reader with excitation at 320 nm and emission at 405 nm. α-Secretase–specific activity was measured as TAPI-I–inhibitable activity.

Immunocytochemistry

For immunocytochemistry, cells were fixed with 4% PFA + 4% sucrose followed by blocking and permeabilization with 2% normal donkey serum plus 0.1% saponin for 1 h. Primary antibodies targeting either A10 (1:200; ab1997, rabbit; Abcam), PS1 (1:1,000; 13A11, mouse), or TFR (both 1:200; ab84036, rabbit [Abcam]; H68.4, mouse [Thermo Fisher Scientific]) were incubated overnight at 4°C in blocking buffer. The following day, cells were washed with PBS and treated with secondary antibody for 1 h at a dilution of 1:2,000 in PBS followed by washes with PBS. Hoechst was included in the second to last wash at a dilution of 1:2,000. All slides were mounted with Vectashield mounting medium (Vector Laboratories). 1-µm optical sections were acquired on a microscope (LSM-710; Carl Zeiss) using a 63× oil immersion objective. All images were processed and analyzed with Zen Black software (Carl Zeiss). To quantify colocalization, all images were stained together in the same session along with control samples where one or both primary antibodies were omitted (to calculate background fluorescence). Automated colocalization analysis of at least 10 images (∼40 cells) was done with Zen Black software according to documented protocols.

Immunohistochemistry on mouse brain tissue

Immunohistochemistry was performed as described previously (Schafer et al., 2012). In brief, 3-mo-old WT C57BL/6 mice were euthanized and perfused with PBS via intracardiac perfusion. Brains were immersed in 4% PFA for 4 h at 4°C, followed by cryoprotection in 30% sucrose/PBS for 48 h. 14-µm sagittal cryosections were cut from optimal cutting temperature compund–embedded brain blocks and stored at −80°C until staining. Slides were dried at 37°C for 20 min to remove condensation, washed twice in PBS, and then blocked with 10% normal goat serum supplemented with 0.3% Triton X-100 for 2 h at room temperature. Primary antibodies were added at a concentration of 1:200 for A10 (PC528; EMD Millipore) and PS1 (13A11) or 1:50 for TFR (ab84036) in blocking buffer overnight at 4°C. The next day, slides were washed three times in PBS for 10 min followed by appropriate Alexa Fluor–conjugated secondary antibodies at a dilution of 1:200 and supplemented with Hoechst (1:2,000) in blocking buffer for 2 h. Slides were washed three times for 30 min and mounted with Vectashield. All images were first checked by confocal microscopy before SIM acquisition.

SIM

For acquiring, processing, and analyzing SIM images on 7W cells and mouse brain tissue, a similar protocol to Hong et al. (2015) was followed. In brief, all samples were imaged using a microscope (ELYRA PS1; Carl Zeiss) with a fixed number of grating rotations (five), and images were processed using the accompanying Zen image acquisition software (Carl Zeiss). For quantification of mouse hippocampal images, the processed 3D SIM images were analyzed by Imaris (bitplane) and MATLAB (MathWorks Inc.) using the spot (ellipsoids) function. Spots were created at the local maxima of all fluorescent puncta spots, and x, y, and z diameters of the ellipsoids were empirically determined for the particular set of antibodies used and confirmed using spot growth boundary so that all spots created appropriately reflected the fluorescent image of each channel. Then, MATLAB was used to determine the number of colocalized spots (≤200-nm distance between spot centers of two channels). The number of colocated spots was then divided by the numbers of spots on the individual channel. All SIM data analysis was done blinded.

FLIM

We performed FLIM according to previously described protocols (Wahlster et al., 2013; Arimon et al., 2015). In brief, to monitor relative proximity between the PS1–γ-secretase and A10–α-secretase in intact cells, 7W cells were immunostained with 13A11 and AB19026 antibodies against PS1 and A10, respectively. The primary antibodies were detected with Alexa Fluor 488 (donor)– and Cy3 (acceptor)- labeled corresponding secondary antibodies. The Alexa Fluor 488 donor fluorophore was excited with a Ti:Sapphire laser (Chameleon; Coherent). Images were taken with a microscope (LSM-510; Carl Zeiss) using a 63× oil immersion objective, and lifetimes were recorded using a high-speed photomultiplier tube (MCP R3809;

Hamamatsu Photonics) and a fast time-correlated single-photon counting acquisition board (SPC-830; Becker & Hickl). All data were analyzed using SPC Image software (Becker & Hickl) where individual cells were outlined and mean donor fluorophore lifetime per cell was quantitated. First, to determine the native lifetime of the donor fluorophore (t1; no FRET), a one-component analysis was used in the donor fluorophore–only immunostained cells (13A11–Alexa Fluor 488). Next, donor- and acceptor-labeled cells were analyzed with a two-component analysis, where t1 was fixed ("excluded") and a new, shorter lifetime of the donor fluorophore (t2), because of the presence of FRET, was determined. The FRET efficiency (E_{FRET}) was calculated using the following equation: $E_{FRET} = (t1 - t2)/t1 \times 100\%$.

ELISA

For Aβ, an Aβ1-40 ELISA (Invitrogen) was performed according to the manufacturer's specifications. Samples were diluted 1:25 to allow detection within the standard range. Alternatively, for certain CM samples, a meso scale discovery (MSD) Aβ triplex ELISA was performed with samples diluted 1:5. For APPs, an MSD duplex ELISA that measures APPs-α and APPs-β was performed as described previously (Hong et al., 2011; Rice et al., 2012) with samples diluted 1:10 per the manufacturer's protocol. In brief, plates were blocked with 3% blocker A for 60 min followed by incubation with samples and standards for 60 min. Plates were washed three times before the addition of detection antibody for 60 min, followed by another three washes. Read buffer was added for 10 min and analyzed on an MSD imager (Sector). All incubations (except read buffer) were done with vigorous shaking on a titer plate shaker.

Quantification and statistical analysis

All quantifications were performed using an infrared imaging system (Odyssey) or using ImageJ software (National Institutes of Health; when blots were performed by ECL detection). For APPs-α, Western blots using an APPs-α–specific antibody, 1736 or 6E10, were quantitated by LI-COR Biosciences. For APPs-β, an MSD ELISA was performed with specific standards. In most cases, data were normalized to controls that were set to 100%. For statistical analysis, a Student's *t* test or one-way or two-way analysis of variance (ANOVA) was used when appropriate; significance was designated at $P < 0.05$.

Online supplemental material

Fig. S1 shows additional surface biotinylation and coIP data demonstrating cell surface interaction between A10 or TACE with γ-secretase. Fig. S2 shows additional imaging data and quantitation by confocal and SIM. Fig. S3 characterizes the phenomenon of γ inhibition on APPs-α secretion. Fig. S4 demonstrates that modulation of γ-secretase by sulindac sulfide or by FAD-causing mutations in PS1 does not alter APPs-α secretion. Fig. S5 shows that γ inhibition does not increase the coIP between A10 and γ-secretase even though it increases APPs-α secretion. Online supplemental material is available at http://www.jcb.org/cgi/content/full/jcb.201502001/DC1.

Acknowledgments

We thank S. Svirsky and O. Berezovska for assistance with FLIM. We are grateful to members of the Selkoe laboratory for helpful discussions.

This research is supported by a BrightFocus grant (A2011648), a National Institutes of Health T32 institutional training grant (AG000222-19 to A.C. Chen), and a National Institute on Aging Program Project grant (AG015379 to D.J. Selkoe).

The authors declare no competing financial interests.

Submitted: 2 February 2015
Accepted: 11 November 2015

References

Arduise, C., T. Abache, L. Li, M. Billard, A. Chabanon, A. Ludwig, P. Mauduit, C. Boucheix, E. Rubinstein, and F. Le Naour. 2008. Tetraspanins regulate ADAM10-mediated cleavage of TNF-α and epidermal growth factor. *J. Immunol.* 181:7002–7013. http://dx.doi.org/10.4049/jimmunol.181.10.7002

Arimon, M., S. Takeda, K.L. Post, S. Svirsky, B.T. Hyman, and O. Berezovska. 2015. Oxidative stress and lipid peroxidation are upstream of amyloid pathology. *Neurobiol. Dis.* 84:109–119. http://dx.doi.org/10.1016/j.nbd.2015.06.013

Brown, M.S., J. Ye, R.B. Rawson, and J.L. Goldstein. 2000. Regulated intramembrane proteolysis: a control mechanism conserved from bacteria to humans. *Cell.* 100:391–398. http://dx.doi.org/10.1016/S0092-8674(00)80675-3

Buxbaum, J.D., K.N. Liu, Y. Luo, J.L. Slack, K.L. Stocking, J.J. Peschon, R.S. Johnson, B.J. Castner, D.P. Cerretti, and R.A. Black. 1998. Evidence that tumor necrosis factor α converting enzyme is involved in regulated α-secretase cleavage of the Alzheimer amyloid protein precursor. *J. Biol. Chem.* 273:27765–27767. http://dx.doi.org/10.1074/jbc.273.43.27765

Cacquevel, M., L. Aeschbach, P. Osenkowski, D. Li, W. Ye, M.S. Wolfe, H. Li, D.J. Selkoe, and P.C. Fraering. 2008. Rapid purification of active γ-secretase, an intramembrane protease implicated in Alzheimer's disease. *J. Neurochem.* 104:210–220.

Chen, A.C., L.Y. Guo, B.L. Ostaszewski, D.J. Selkoe, and M.J. LaVoie. 2010. Aph-1 associates directly with full-length and C-terminal fragments of γ-secretase substrates. *J. Biol. Chem.* 285:11378–11391. http://dx.doi.org/10.1074/jbc.M109.088815

Chyung, J.H., D.M. Raper, and D.J. Selkoe. 2005. γ-secretase exists on the plasma membrane as an intact complex that accepts substrates and effects intramembrane cleavage. *J. Biol. Chem.* 280:4383–4392. http://dx.doi.org/10.1074/jbc.M409272200

Citron, M., D. Westaway, W. Xia, G. Carlson, T. Diehl, G. Levesque, K. Johnson-Wood, M. Lee, P. Seubert, A. Davis, et al. 1997. Mutant presenilins of Alzheimer's disease increase production of 42-residue amyloid beta-protein in both transfected cells and transgenic mice. *Nat. Med.* 3:67–72. http://dx.doi.org/10.1038/nm0197-67

De Strooper, B. 2003. Aph-1, Pen-2, and Nicastrin with Presenilin generate an active γ-Secretase complex. *Neuron.* 38:9–12. http://dx.doi.org/10.1016/S0896-6273(03)00205-8

De Strooper, B., W. Annaert, P. Cupers, P. Saftig, K. Craessaerts, J.S. Mumm, E.H. Schroeter, V. Schrijvers, M.S. Wolfe, W.J. Ray, et al. 1999. A presenilin-1-dependent γ-secretase-like protease mediates release of Notch intracellular domain. *Nature.* 398:518–522. http://dx.doi.org/10.1038/19083

Doody, R.S., R. Raman, M. Farlow, T. Iwatsubo, B. Vellas, S. Joffe, K. Kieburtz, F. He, X. Sun, R.G. Thomas, et al. 2013. A phase 3 trial of semagacestat for treatment of Alzheimer's disease. *N. Engl. J. Med.* 369:341–350. http://dx.doi.org/10.1056/NEJMoa1210951

Dornier, E., F. Coumailleau, J.F. Ottavi, J. Moretti, C. Boucheix, P. Mauduit, F. Schweisguth, and E. Rubinstein. 2012. TspanC8 tetraspanins regulate ADAM10/Kuzbanian trafficking and promote Notch activation in flies and mammals. *J. Cell Biol.* 199:481–496. http://dx.doi.org/10.1083/jcb.201201133

Dunn, C.D., M.L. Sulis, A.A. Ferrando, and I. Greenwald. 2010. A conserved tetraspanin subfamily promotes Notch signaling in *Caenorhabditis elegans* and in human cells. *Proc. Natl. Acad. Sci. USA.* 107:5907–5912. http://dx.doi.org/10.1073/pnas.1001647107

Edbauer, D., E. Winkler, C. Haass, and H. Steiner. 2002. Presenilin and nicastrin regulate each other and determine amyloid β-peptide production via complex formation. *Proc. Natl. Acad. Sci. USA.* 99:8666–8671. http://dx.doi.org/10.1073/pnas.132277899

Esler, W.P., W.T. Kimberly, B.L. Ostaszewski, W. Ye, T.S. Diehl, D.J. Selkoe, and M.S. Wolfe. 2002. Activity-dependent isolation of the presenilin–γ-secretase complex reveals nicastrin and a γ substrate. *Proc. Natl. Acad. Sci. USA.* 99:2720–2725. http://dx.doi.org/10.1073/pnas.052436599

Esselens, C., R. Sannerud, R. Gallardo, V. Baert, D. Kaden, L. Serneels, B. De Strooper, F. Rousseau, G. Multhaup, J. Schymkowitz, et al. 2012. Peptides based on the presenilin-APP binding domain inhibit APP processing and Aβ production through interfering with the APP transmembrane domain. *FASEB J.* 26:3765–3778. http://dx.doi.org/10.1096/fj.11-201368

Evin, G., L.D. Canterford, D.E. Hoke, R.A. Sharples, J.G. Culvenor, and C.L. Masters. 2005. Transition-state analogue γ-secretase inhibitors stabilize a 900 kDa presenilin/nicastrin complex. *Biochemistry.* 44:4332–4341. http://dx.doi.org/10.1021/bi0481702

Greenwald, I. 2012. Notch and the awesome power of genetics. *Genetics.* 191:655–669. http://dx.doi.org/10.1534/genetics.112.141812

Gutwein, P., S. Mechtersheimer, S. Riedle, A. Stoeck, D. Gast, S. Joumaa, H. Zentgraf, M. Fogel, and D.P. Altevogt. 2003. ADAM10-mediated cleavage of L1 adhesion molecule at the cell surface and in released membrane vesicles. *FASEB J.* 17:292–294.

Haass, C., M.G. Schlossmacher, A.Y. Hung, C. Vigo-Pelfrey, A. Mellon, B.L. Ostaszewski, I. Lieberburg, E.H. Koo, D. Schenk, D.B. Teplow, et al. 1992. Amyloid β-peptide is produced by cultured cells during normal metabolism. *Nature.* 359:322–325. http://dx.doi.org/10.1038/359322a0

Haining, E.J., J. Yang, R.L. Bailey, K. Khan, R. Collier, S. Tsai, S.P. Watson, J. Frampton, P. Garcia, and M.G. Tomlinson. 2012. The TspanC8 subgroup of tetraspanins interacts with A disintegrin and metalloprotease 10 (ADAM10) and regulates its maturation and cell surface expression. *J. Biol. Chem.* 287:39753–39765. http://dx.doi.org/10.1074/jbc.M112.416503

Hardy, J., and D.J. Selkoe. 2002. The amyloid hypothesis of Alzheimer's disease: progress and problems on the road to therapeutics. *Science.* 297:353–356. http://dx.doi.org/10.1126/science.1072994

Hébert, S.S., L. Serneels, T. Dejaegere, K. Horré, M. Dabrowski, V. Baert, W. Annaert, D. Hartmann, and B. De Strooper. 2004. Coordinated and widespread expression of γ-secretase in vivo: evidence for size and molecular heterogeneity. *Neurobiol. Dis.* 17:260–272. http://dx.doi.org/10.1016/j.nbd.2004.08.002

Hemming, M.L., J.E. Elias, S.P. Gygi, and D.J. Selkoe. 2008. Proteomic profiling of γ-secretase substrates and mapping of substrate requirements. *PLoS Biol.* 6:e257. http://dx.doi.org/10.1371/journal.pbio.0060257

Herl, L., A.V. Thomas, C.M. Lill, M. Banks, A. Deng, P.B. Jones, R. Spoelgen, B.T. Hyman, and O. Berezovska. 2009. Mutations in amyloid precursor protein affect its interactions with presenilin/γ-secretase. *Mol. Cell. Neurosci.* 41:166–174. http://dx.doi.org/10.1016/j.mcn.2009.02.008

Hong, S., O. Quintero-Monzon, B.L. Ostaszewski, D.R. Podlisny, W.T. Cavanaugh, T. Yang, D.M. Holtzman, J.R. Cirrito, and D.J. Selkoe. 2011. Dynamic analysis of amyloid β-protein in behaving mice reveals opposing changes in ISF versus parenchymal Aβ during age-related plaque formation. *J. Neurosci.* 31:15861–15869. http://dx.doi.org/10.1523/JNEUROSCI.3272-11.2011

Hong, S., D. Wilton, B. Stevens, and D. Richardson. 2015. Structured illumination microscopy for the investigation of synaptic structure and function. *In* Methods in Molecular Biology. J.M. Walker, editor. Springer-Verlag New York Inc., New York. In press.

Hur, J.Y., Y. Teranishi, T. Kihara, N.G. Yamamoto, M. Inoue, W. Hosia, M. Hashimoto, B. Winblad, S. Frykman, and L.O. Tjernberg. 2012. Identification of novel γ-secretase-associated proteins in detergent-resistant membranes from brain. *J. Biol. Chem.* 287:11991–12005. http://dx.doi.org/10.1074/jbc.M111.246074

Jurisch-Yaksi, N., R. Sannerud, and W. Annaert. 2013. A fast growing spectrum of biological functions of γ-secretase in development and disease. *Biochim. Biophys. Acta.* 1828:2815–2827. http://dx.doi.org/10.1016/j.bbamem.2013.04.016

Kaether, C., S. Lammich, D. Edbauer, M. Ertl, J. Rietdorf, A. Capell, H. Steiner, and C. Haass. 2002. Presenilin-1 affects trafficking and processing of βAPP and is targeted in a complex with nicastrin to the plasma membrane. *J. Cell Biol.* 158:551–561. http://dx.doi.org/10.1083/jcb.200201123

Kimberly, W.T., M.J. LaVoie, B.L. Ostaszewski, W. Ye, M.S. Wolfe, and D.J. Selkoe. 2003. γ-Secretase is a membrane protein complex comprised of presenilin, nicastrin, Aph-1, and Pen-2. *Proc. Natl. Acad. Sci. USA.* 100:6382–6387. http://dx.doi.org/10.1073/pnas.1037392100

Koo, E.H., S.L. Squazzo, D.J. Selkoe, and C.H. Koo. 1996. Trafficking of cell-surface amyloid beta-protein precursor. I. Secretion, endocytosis and recycling as detected by labeled monoclonal antibody. *J. Cell Sci.* 109:991–998.

Kuhn, P.H., H. Wang, B. Dislich, A. Colombo, U. Zeitschel, J.W. Ellwart, E. Kremmer, S. Rossner, and S.F. Lichtenthaler. 2010. ADAM10 is the physiologically relevant, constitutive α-secretase of the amyloid precursor protein in primary neurons. *EMBO J.* 29:3020–3032. http://dx.doi.org/10.1038/emboj.2010.167

LaVoie, M.J., P.C. Fraering, B.L. Ostaszewski, W. Ye, W.T. Kimberly, M.S. Wolfe, and D.J. Selkoe. 2003. Assembly of the γ-secretase complex involves early formation of an intermediate subcomplex of Aph-1 and nicastrin. *J. Biol. Chem.* 278:37213–37222. http://dx.doi.org/10.1074/jbc.M303941200

Li, Y.M., M.T. Lai, M. Xu, Q. Huang, J. DiMuzio-Mower, M.K. Sardana, X.P. Shi, K.C. Yin, J.A. Shafer, and S.J. Gardell. 2000. Presenilin 1 is linked with γ-secretase activity in the detergent solubilized state. *Proc. Natl. Acad. Sci. USA.* 97:6138–6143. http://dx.doi.org/10.1073/pnas.110126897

Lleó, A., O. Berezovska, L. Herl, S. Raju, A. Deng, B.J. Bacskai, M.P. Frosch, M. Irizarry, and B.T. Hyman. 2004. Nonsteroidal anti-inflammatory drugs lower $A_{\beta 42}$ and change presenilin 1 conformation. *Nat. Med.* 10:1065–1066. http://dx.doi.org/10.1038/nm1112

Manders, E.M., J. Stap, G.J. Brakenhoff, R. van Driel, and J.A. Aten. 1992. Dynamics of three-dimensional replication patterns during the S-phase, analysed by double labelling of DNA and confocal microscopy. *J. Cell Sci.* 103:857–862.

Muratore, C.R., H.C. Rice, P. Srikanth, D.G. Callahan, T. Shin, L.N. Benjamin, D.M. Walsh, D.J. Selkoe, and T.L. Young-Pearse. 2014. The familial Alzheimer's disease APPV717I mutation alters APP processing and Tau expression in iPSC-derived neurons. *Hum. Mol. Genet.* 23:3523–3536. http://dx.doi.org/10.1093/hmg/ddu064

Osenkowski, P., H. Li, W. Ye, D. Li, L. Aeschbach, P.C. Fraering, M.S. Wolfe, D.J. Selkoe, and H. Li. 2009. Cryoelectron microscopy structure of purified γ-secretase at 12 Å resolution. *J. Mol. Biol.* 385:642–652. http://dx.doi.org/10.1016/j.jmb.2008.10.078

Podlisny, M.B., D.R. Tolan, and D.J. Selkoe. 1991. Homology of the amyloid beta protein precursor in monkey and human supports a primate model for beta amyloidosis in Alzheimer's disease. *Am. J. Pathol.* 138:1423–1435.

Podlisny, M.B., M. Citron, P. Amarante, R. Sherrington, W. Xia, J. Zhang, T. Diehl, G. Levesque, P. Fraser, C. Haass, et al. 1997. Presenilin proteins undergo heterogeneous endoproteolysis between Thr291 and Ala299 and occur as stable N- and C-terminal fragments in normal and Alzheimer brain tissue. *Neurobiol. Dis.* 3:325–337. http://dx.doi.org/10.1006/nbdi.1997.0129

Portelius, E., R.A. Dean, M.K. Gustavsson, U. Andreasson, H. Zetterberg, E. Siemers, and K. Blennow. 2010. A novel Aβ isoform pattern in CSF reflects γ-secretase inhibition in Alzheimer disease. *Alzheimers Res. Ther.* 2:7. http://dx.doi.org/10.1186/alzrt30

Prox, J., M. Willenbrock, S. Weber, T. Lehmann, D. Schmidt-Arras, R. Schwanbeck, P. Saftig, and M. Schwake. 2012. Tetraspanin15 regulates cellular trafficking and activity of the ectodomain sheddase ADAM10. *Cell. Mol. Life Sci.* 69:2919–2932. http://dx.doi.org/10.1007/s00018-012-0960-2

Ray, W.J., M. Yao, J. Mumm, E.H. Schroeter, P. Saftig, M. Wolfe, D.J. Selkoe, R. Kopan, and A.M. Goate. 1999. Cell surface presenilin-1 participates in the γ-secretase-like proteolysis of Notch. *J. Biol. Chem.* 274:36801–36807. http://dx.doi.org/10.1074/jbc.274.51.36801

Rice, H.C., M. Townsend, J. Bai, S. Suth, W. Cavanaugh, D.J. Selkoe, and T.L. Young-Pearse. 2012. Pancortins interact with amyloid precursor protein and modulate cortical cell migration. *Development.* 139:3986–3996. http://dx.doi.org/10.1242/dev.082909

Schafer, D.P., E.K. Lehrman, A.G. Kautzman, R. Koyama, A.R. Mardinly, R. Yamasaki, R.M. Ransohoff, M.E. Greenberg, B.A. Barres, and B. Stevens. 2012. Microglia sculpt postnatal neural circuits in an activity and complement-dependent manner. *Neuron.* 74:691–705. http://dx.doi.org/10.1016/j.neuron.2012.03.026

Schlöndorff, J., J.D. Becherer, and C.P. Blobel. 2000. Intracellular maturation and localization of the tumour necrosis factor alpha convertase (TACE). *Biochem. J.* 347:131–138. http://dx.doi.org/10.1042/bj3470131

Shirotani, K., D. Edbauer, S. Prokop, C. Haass, and H. Steiner. 2004. Identification of distinct γ-secretase complexes with different APH-1 variants. *J. Biol. Chem.* 279:41340–41345. http://dx.doi.org/10.1074/jbc.M405768200

Teranishi, Y., J.Y. Hur, G.J. Gu, T. Kihara, T. Ishikawa, T. Nishimura, B. Winblad, H. Behbahani, M. Kamali-Moghaddam, S. Frykman, and L.O. Tjernberg. 2012. Erlin-2 is associated with active γ-secretase in brain and affects amyloid β-peptide production. *Biochem. Biophys. Res. Commun.* 424:476–481. http://dx.doi.org/10.1016/j.bbrc.2012.06.137

Tousseyn, T., A. Thathiah, E. Jorissen, T. Raemaekers, U. Konietzko, K. Reiss, E. Maes, A. Snellinx, L. Serneels, O. Nyabi, et al. 2009. ADAM10, the rate-limiting protease of regulated intramembrane proteolysis of Notch and other proteins, is processed by ADAMS-9, ADAMS-15, and the γ-secretase. *J. Biol. Chem.* 284:11738–11747. http://dx.doi.org/10.1074/jbc.M805894200

Vassar, R., B.D. Bennett, S. Babu-Khan, S. Kahn, E.A. Mendiaz, P. Denis, D.B. Teplow, S. Ross, P. Amarante, R. Loeloff, et al. 1999. β-secretase cleavage of Alzheimer's amyloid precursor protein by the transmembrane aspartic protease BACE. *Science.* 286:735–741. http://dx.doi.org/10.1126/science.286.5440.735

Wahlster, L., M. Arimon, N. Nasser-Ghodsi, K.L. Post, A. Serrano-Pozo, K. Uemura, and O. Berezovska. 2013. Presenilin-1 adopts pathogenic conformation in normal aging and in sporadic Alzheimer's disease. *Acta Neuropathol.* 125:187–199. http://dx.doi.org/10.1007/s00401-012-1065-6

Wakabayashi, T., K. Craessaerts, L. Bammens, M. Bentahir, F. Borgions, P. Herdewijn, A. Staes, E. Timmerman, J. Vandekerckhove, E. Rubinstein, et al. 2009. Analysis of the γ-secretase interactome and validation of its association with tetraspanin-enriched microdomains. *Nat. Cell Biol.* 11:1340–1346. http://dx.doi.org/10.1038/ncb1978

Weber, S., and P. Saftig. 2012. Ectodomain shedding and ADAMs in development. *Development.* 139:3693–3709. http://dx.doi.org/10.1242/dev.076398

Xia, W., J. Zhang, D. Kholodenko, M. Citron, M.B. Podlisny, D.B. Teplow, C. Haass, P. Seubert, E.H. Koo, and D.J. Selkoe. 1997a. Enhanced production and oligomerization of the 42-residue amyloid β-protein by Chinese hamster ovary cells stably expressing mutant presenilins. *J. Biol. Chem.* 272:7977–7982. http://dx.doi.org/10.1074/jbc.272.12.7977

Xia, W., J. Zhang, R. Perez, E.H. Koo, and D.J. Selkoe. 1997b. Interaction between amyloid precursor protein and presenilins in mammalian cells: implications for the pathogenesis of Alzheimer disease. *Proc. Natl. Acad. Sci. USA.* 94:8208–8213. http://dx.doi.org/10.1073/pnas.94.15.8208

Xu, D., C. Sharma, and M.E. Hemler. 2009. Tetraspanin12 regulates ADAM10-dependent cleavage of amyloid precursor protein. *FASEB J.* 23:3674–3681. http://dx.doi.org/10.1096/fj.09-133462

Yu, G., F. Chen, G. Levesque, M. Nishimura, D.M. Zhang, L. Levesque, E. Rogaeva, D. Xu, Y. Liang, M. Duthie, et al. 1998. The presenilin 1 protein is a component of a high molecular weight intracellular complex that contains β-catenin. *J. Biol. Chem.* 273:16470–16475. http://dx.doi.org/10.1074/jbc.273.26.16470

Zhou, S., H. Zhou, P.J. Walian, and B.K. Jap. 2005. CD147 is a regulatory subunit of the γ-secretase complex in Alzheimer's disease amyloid β-peptide production. *Proc. Natl. Acad. Sci. USA.* 102:7499–7504. http://dx.doi.org/10.1073/pnas.0502768102